https://doi.org/10.1093/plphys/kiad049 PLANT PHYSIOLOGY 2023: 192: 1289–1306

Plant Physiology®

Research Article

Natural overexpression of *CAROTENOID CLEAVAGE DIOXYGENASE 4* in tomato alters carotenoid flux

Hee Ju Yoo,[1] Mi-Young Chung,[2] Hyun-Ah Lee,[3] Soo-Bin Lee,[1] Silvana Grandillo,[4] James J. Giovannoni[5] and Je Min Lee[1,*]

1 Department of Horticultural Science, Kyungpook National University, Daegu 41566, Korea
2 Department of Agricultural Education, Sunchon National University, Suncheon 57922, Korea
3 Division of Eco-Friendly Horticulture, Yonam College, Cheonan 31005, Korea
4 CNR-Institute of Bioscience and Bioresources (IBBR), Via Università 133, 80055 Portici, Italy
5 Boyce Thompson Institute and USDA-ARS Robert W. Holley Center, Tower Rd., Cornell University Campus, Ithaca, NY 14853, USA

*Author for correspondence: jemin@knu.ac.kr (J. M. L.)
The author responsible for distribution of materials integral to the findings presented in this article in accordance with the policy described in the Instructions for Authors (https://academic.oup.com/plphys/pages/General-Instructions) is: Je Min Lee.

Abstract

Carotenoids and apocarotenoids function as pigments and flavor volatiles in plants that enhance consumer appeal and offer health benefits. Tomato (*Solanum lycopersicum*.) fruit, especially those of wild species, exhibit a high degree of natural variation in carotenoid and apocarotenoid contents. Using positional cloning and an introgression line (IL) of *Solanum habrochaites* "LA1777', IL8A, we identified carotenoid cleavage dioxygenase 4 (CCD4) as the factor responsible for controlling the dark orange fruit color. *CCD4b* expression in ripe fruit of IL8A plants was ~8,000 times greater than that in the wild type, presumably due to 5′ *cis*-regulatory changes. The ShCCD4b-GFP fusion protein localized in the plastid. Phytoene, ζ-carotene, and neurosporene levels increased in *ShCCD4b*-overexpressing ripe fruit, whereas *trans*-lycopene, β-carotene, and lutein levels were reduced, suggestive of feedback regulation in the carotenoid pathway by an unknown apocarotenoid. Solid-phase microextraction–gas chromatography–mass spectrometry analysis showed increased levels of geranylacetone and β-ionone in *ShCCD4b*-overexpressing ripe fruit coupled with a β-cyclocitral deficiency. In carotenoid-accumulating *Escherichia coli* strains, ShCCD4b cleaved both ζ-carotene and β-carotene at the C9–C10 (C9′–C10′) positions to produce geranylacetone and β-ionone, respectively. Exogenous β-cyclocitral decreased carotenoid synthesis in the ripening fruit of tomato and pepper (*Capsicum annuum*), suggesting feedback inhibition in the pathway. Our findings will be helpful for enhancing the aesthetic and nutritional value of tomato and for understanding the complex regulatory mechanisms of carotenoid and apocarotenoid biogenesis.

Introduction

Carotenoids are integral for light harvesting and photosynthesis, as well as photoprotection from photooxidative damage under excess light conditions. Carotenoids provide sources of pigment variation in reproductive organs to attract seed dispersers and pollinators. Carotenoids also play important roles in human health as antioxidants, reducing the risk of various diseases such as cancers and eye diseases (Krinsky et al. 2003, Krinsky and Johnson 2005). The oxidative breakage of carotenoids results in the formation of a diverse family of essential metabolites, known as apocarotenoids.

Apocarotenoids are primarily derived by cleavage of carotenoids at a specific conjugated double bond (Mein et al. 2011, Ramel et al. 2012, Liang et al. 2018). Carotenoid cleavage dioxygenase (CCD)-mediated catabolism is the primary enzymatic pathway to generate diverse apocarotenoids from carotenoids. CCDs are divided into 2 groups: 9-*cis*-epoxycarotenoid cleavage dioxygenases (NCEDs) and

Received November 08, 2022. Accepted December 26, 2022. Advance access publication January 30, 2023
© American Society of Plant Biologists 2023. All rights reserved. For permissions, please e-mail: journals.permissions@oup.com

Downloaded from https://academic.oup.com/plphys/article/192/2/1289/7009207 by Biblioteca Centrale Agraria user on 16 June 2023

CCDs. In plants, there are 5 NCEDs (NCED2, 3, 5, 6, and 9) and 6 CCDs (CCD1, 2, 4, 7, 8, and 10) (Frusciante et al. 2014, Ahrazem et al. 2016a, Zhong et al. 2020). The NCEDs cleave 9-*cis*-epoxycarotenoids, including 9-*cis*-violaxanthin and 9-*cis*-neoxanthin at the C11–C12 double bond, to produce xanthoxin, an abscisic acid (ABA) precursor (Schwartz et al. 1997, Tan et al. 2003). The CCDs have different substrate specificity and cleavage sites, producing various apocarotenoids. CCD1 has a relaxed substrate specificity and cleaves at the C5–C6 (C5′–C6′), C7–C8 (C7′–C8′), and C9–C10 (C9′–C10′) double bonds to generate various apocarotenoids (Ibdah et al. 2006, Schmidt et al. 2006, Vogel et al. 2008, Ilg et al. 2014). CCD2 produces crocetin dialdehyde and controls red stigma pigmentation by cleaving zeaxanthin at the C7′–C8′ double bond in saffron (*Crocus sativus*) (Frusciante et al. 2014). This enzyme, similar to members of the related CCD1 subfamily, appears to be localized in the plastid, unlike cytosol-targeted CCD1. CCD7 and CCD8 are associated with strigolactone synthesis (Schwartz et al. 2004, Kohlen et al. 2012). All-*trans*-β-carotene is converted to 9-*cis*-β-carotene by β-carotene isomerase D27 (Alder et al. 2012), and CCD7 cleaves 9-*cis*-β-carotene at the C9′–C10′ double bond to produce β-ionone and 9-*cis*-β-apo-10′-carotenal. Subsequently, CCD8 catalyzes the cleavage of 9-*cis*-β-apo-10′-carotenal at the C13–C14 double bond to yield carlactone, a precursor of strigolactone (Vogel et al. 2010b, Kohlen et al. 2012). AtCCD7 cleaves 9-*cis*-configured acyclic carotene at the C9–C10 double bond and is proposed to generate acyclic retrograde signals (Bruno et al. 2016). CCD10 in maize (*Zea mays*) (ZmCCD10a) cleaves phytoene, lycopene, δ-carotene, ε-carotene, and β-carotene at the C5–C6 (C5′–C6′) and C9–C10 (C9′–C10′) to produce geranylacetone, 6-methyl-5-hepten-2-one (MHO), α-ionone, and β-ionone (Zhong et al. 2020) (Fig. 1).

Like CCD1, CCD4 typically shows broad substrate specificity and commonly cleaves carotenoids at the C5–C6 (C5′–C6′), C7–C8 (C7′–C8′), and C9–C10 (C9′–C10′) positions, producing diverse apocarotenoids (Ahrazem et al. 2016a). AtCCD4 specifically cleaves all-*trans*-configured cyclic carotenoids at the C9–C10 (C9′–C10′) positions (Bruno et al. 2016). Altered *CCD4* expression can influence organ pigmentation. Downregulation of *CmCCD4a* and *StCCD4* increases carotenoid contents and causes a yellow color change in chrysanthemum (*Chrysanthemum morifolium*) flowers and potato (*Solanum tuberosum*) tubers, respectively (Ohmiya et al. 2006, Campbell et al. 2010). *CCD4* silencing in the white flesh of peaches (*Prunus persica*) results in yellow flesh due to increased carotenoid contents (Bai et al. 2015). Insertion of CACTA-like transposable element 1 in the *BnaC3.CCD4* open reading frame downregulates its expression, changing the flower color from white to yellow in *Brassica* species (Zhang et al. 2015). In citrus fruits (*Citrus clementina* and *Citrus unshiu*), overexpression of *CCD4* increases the red pigment, β-citraurin, in the flavedo (Ma et al. 2013, Rodrigo et al. 2013, Zheng et al. 2019).

Apocarotenoids have various biological functions in plants and animals (von Lintig and Vogt 2004, Hou et al. 2016). For example, retinal—a protein-binding rhodopsin chromophore—converts light to metabolic energy (Kloer et al. 2005). Retinol (vitamin A) and retinoic acid are important nutrients in animals including humans. β-Ionone has anticancer activities in various tumor cells (Liu et al. 2008, Ansari and Emami 2016). In plants, ABA and strigolactone are important apocarotenoid hormones controlling development and stress responses (Schwartz et al. 1997, Sharp et al. 2000, Dun et al. 2009, Zhang et al. 2018). Beyond the well-known function of ABA as a stress hormone, it contributes to increased fruit firmness and an extended fruit shelf life (Diretto et al. 2020). Strigolactone inhibits shoot branching involved in axillary bud outgrowth (Umehara et al. 2008) and, as a root-derived signal, interacts with symbiotic arbuscular mycorrhizal fungi to assist with the uptake of nutrients from soil to plant (Waters et al. 2017). Apocarotenoid signals (ACSs) (Hou et al. 2016)—or uncharacterized linear *cis*-carotene-derived apocarotenoids (Moreno et al. 2021)—were proposed to control plant development and physiology. ACS1 and ACS2 derived from linear *cis*-carotenoids are related to chloroplast biogenesis in Arabidopsis (*Arabidopsis thaliana*) leaves (Avendano-Vazquez et al. 2014) and carotenoid feedback regulation in tomato (*Solanum lycopersicum*) fruits (Kachanovsky et al. 2012). ACS3 derived from the β branch of carotene biosynthesis—presumably from β-carotene—regulates root development in Arabidopsis seedlings (Van Norman et al. 2014). In addition, β-cyclocitral, zaxinone, and anchorene are signaling molecules involved in plant growth, development, stress response, and carotenoid feedback regulation (Moreno et al. 2021). β-Cyclocitral helps to adjust oxidative stress caused by high-light conditions (D'Alessandro et al. 2018). In Arabidopsis, tomato, and rice (*Oryza sativa*), β-cyclocitral increases primary and lateral root growth by inducing cell division under normal and salt stress conditions (Dickinson et al. 2019). Increased reactive oxygen species by wounding and simulated herbivory in Arabidopsis leaves causes the conversion of β-carotene to β-cyclocitral, leading to direct inhibition of 1-deoxy-D-xylulose 5-phosphate synthase (DXS) activity (Mitra et al. 2021). Retinal and its binding protein, lipocalin, regulate the root clock in Arabidopsis (Dickinson et al. 2021).

Apocarotenoid volatiles are vital flavor components in economically important crops (Klee 2010). The contents of flavor volatiles are typically substantially lower in cultivated tomato varieties than in heirloom varieties. Loss of flavor in cultivated tomato (*Solanum lycopersicum*) is associated with diminished production of sugars and volatile precursors, including fatty acids, amino acids, and carotenoids (Goff and Klee 2006). Volatile apocarotenoids act as aromas in flowers and as flavors in fruits (Lewinsohn et al. 2005). Volatile apocarotenoids, including geranylacetone, MHO, β-ionone, and β-damascenone, affect the perception of sweetness as fruity/floral flavors (Mathieu et al. 2009, Vogel et al. 2010a,

Downloaded from https://academic.oup.com/plphys/article/192/2/1289/7009207 by Biblioteca Centrale Agraria user on 16 June 2023

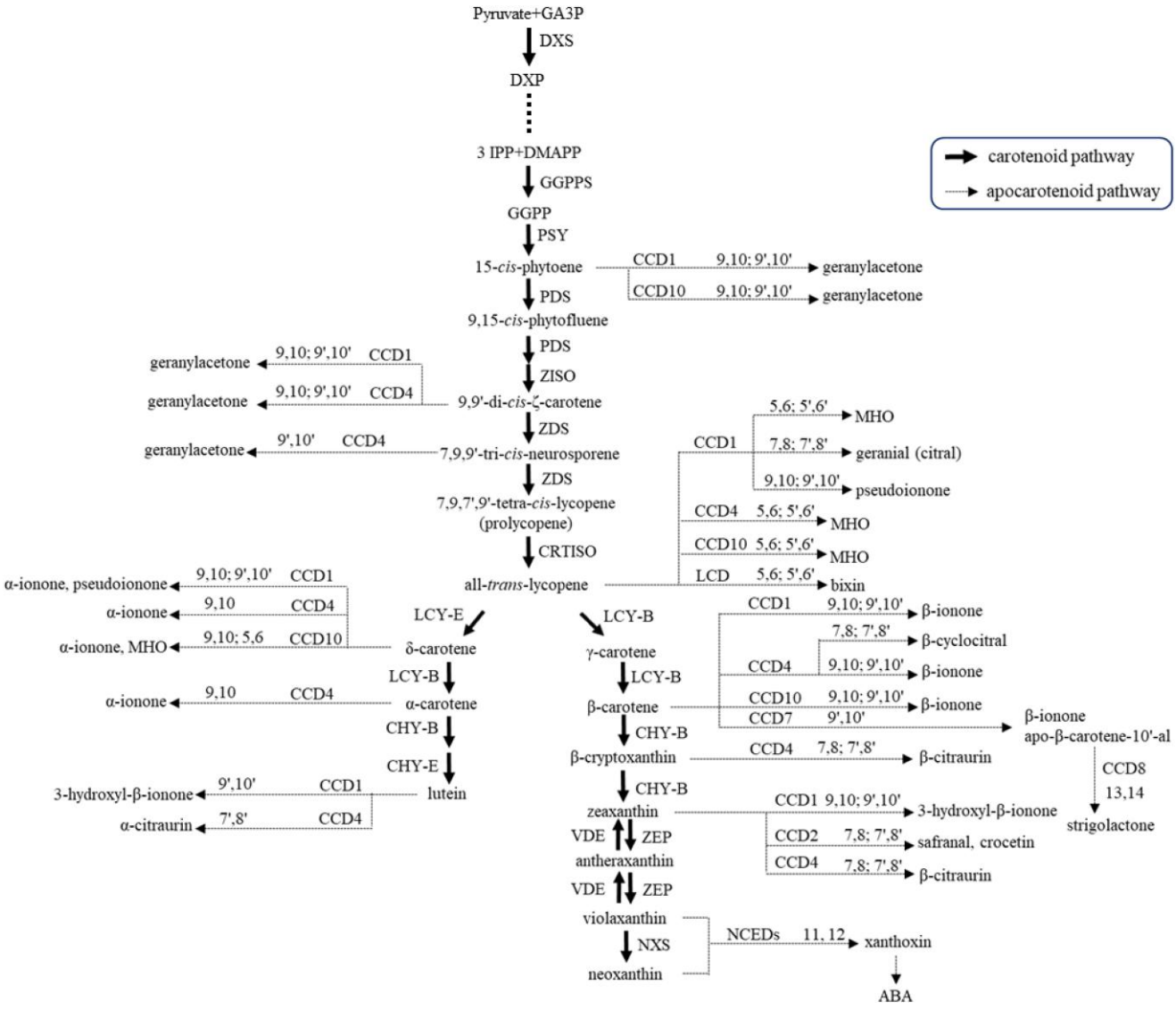

Figure 1 Carotenoid and apocarotenoid biosynthetic pathway. Bold arrows indicate the carotenoid biosynthetic pathway, and dotted-line arrows indicate the apocarotenoid biosynthetic pathway. GA3P, glyceraldehyde 3-phosphate; DXP, 1-deoxy-D-xylulose 5-phosphate; DXS, DXP synthase; IPP, isopentenyl diphosphate; DMAPP, dimethylallyl diphosphate; GGPP, geranylgeranyl diphosphate; GGPPS, geranylgeranyl diphosphate synthase; PSY, phytoene synthase; PDS, phytoene desaturase; ZISO, ζ-carotene isomerase; ZDS, ζ-carotene desaturase; CRTISO, carotene isomerase; LCY-E, lycopene ϵ-cyclase; LCY-B, lycopene β-cyclase; CHY-B, β-carotene hydroxylase; CHY-E, ϵ-ring hydroxylase; ZEP, zeaxanthin epoxidase; VDE, violaxanthin de-epoxidase; NXS, neoxanthin synthase; CCD, carotenoid cleavage dioxygenase; NCED, nine-*cis*-epoxycarotenoid dioxygenase; MHO, 6-methyl-5-hepten-2-one; ABA, abscisic acid.

Klee and Tieman 2018). Fruit sugar level as a primary factor of flavor is negatively associated with yield and/or fruit size (Tieman et al. 2017). Therefore, alternative approaches to improve fruit quality without yield penalty are being investigated. Because volatiles are essential to fruit flavor, identifying the genetic determinants of flavor volatiles is of great interest.

Tomato is one of the most widely cultivated and economically important crops in the world. Because there is little genetic variation among cultivated tomatoes, wild species have been exploited for improving many traits, including fruit quality (Monforte and Tanksley 2000, Zamir 2001). To better exploit genetic variations among wild species, a library of introgression lines (ILs) was developed and is well used (Schauer et al. 2006, Lippman et al. 2007). Wild species including *S. pennellii*, *S. lycopersicoides*, and *S. habrochaites* were used to develop these libraries (Chetelat and Meglic 2000, Monforte and Tanksley 2000, Zamir 2001). The ILs have been used to investigate genetic factors controlling agriculturally valuable traits including carotenoid contents, yield, disease resistance, and volatile compounds (Eshed and Zamir 1995, Zamir 2001, Tieman et al. 2006). *S. habrochaites* contains wide genetic variation, including genes for cold tolerance, dense trichomes, insect resistance, and diverse metabolisms (Monforte and Tanksley 2000, Fan et al. 2019).

Downloaded from https://academic.oup.com/plphys/article/192/2/1289/7009207 by Biblioteca Centrale Agraria user on 16 June 2023

In this study, the overexpression of *ShCCD4b* from *S. habrochaites* was identified as a genetic determinant of dark orange fruit color and apocarotenoid flavors.

Results

Positional cloning of genes regulating the dark orange fruit color in IL8A

IL8A (an *S. habrochaites* "LA1777' IL) has dark orange fruit, whereas *S. lycopersicum* "E6203' has red fruit (Fig. 2A). We analyzed carotenoids in ripe fruit of both lines harvested at 10 d postbreaker (B + 10; Fig. 2B). The total carotenoid content in ripe fruit of IL8A (36.45 $\mu g \cdot g^{-1}$ FW) was 4-fold lower than that of E6203 (147.00 $\mu g \cdot g^{-1}$ FW). In IL8A, the level of *trans*-lycopene was decreased, and β-carotene and lutein were not detected. Levels of phytoene, phytofluene, and ζ-carotene were not significantly changed. These findings suggest that reduced amounts of lycopene, β-carotene, and lutein result in the dark orange fruit of IL8A.

The ripe fruit color of 212 F_2 plants derived from a cross between E6203 and IL8A segregated with a 3:1 ratio (162 dark orange and 50 red; $\chi^2 = 0.2264$, $P = 0.6342$), indicating that dark orange fruit color is controlled by a single dominant gene.

To identify the gene responsible for regulating fruit color of IL8A, map-based cloning was conducted using the E6203 × IL8A F_2 population (Fig. 3A). In IL8A, an introgressed chromosomal segment from LA1777 was identified using markers c (57.3 Mb) and m (60.1 Mb) on chromosome 8 (Supplemental Table S1). F_2 plants were screened with 15 markers from 56.3 to 60.4 Mb, and 27 recombinant plants were found, indicative of a recombination hot spot. The candidate region was delimited to the genomic region between markers h and i, which spanned ~140 kb (59.5–59.6 Mb; ITAG 2.4 gene model) containing 13 genes (Supplemental Table S2). Among these genes, 2 *CCDs*—*SlCCD4a* and *SlCCD4b*—were tandemly duplicated within ~20 kb. CCD4 cleaves carotenoids to produce apocarotenoids in many plants (Huang et al. 2009). The expression of *CCD4b* in ripe fruit was ~8000-fold higher in IL8A than in E6203, based on reverse transcription quantitative PCR (RT-qPCR) analysis using conserved primers of *SlCCD4b* and *ShCCD4b*, whereas expression of *CCD4a* and other linked genes was not significantly difference at $P < 0.05$ and $P < 0.01$ according to independent *t*-test (Fig. 3B; Supplemental Fig. S1). Therefore, *SlCCD4b* was selected as a candidate gene for regulating the carotenoid variation in IL8A.

Identifying natural CCD4b variations in tomato

SlCCD4b (Solc08g075490) encodes a protein of 594 amino acids and contains a plastid transit peptide at the N terminus. ShCCD4b showed 98.65% and 76.92% identity with SlCCD4b and SlCCD4a, respectively. *ShCCD4b* contained 34 nucleotide variations in the coding region, leading to 6 amino acid substitutions and one deletion; there were 25 variations within an ~2.5-kb promoter region of *ShCCD4b* compared with *SlCCD4b* (Fig. 3C). Functional motifs required for CCD activity, such as the 4 histidine residues coordinating with the Fe^{2+} cofactor and aspartate or glutamate residues holding histidine, were conserved in ShCCD4b and SlCCD4b

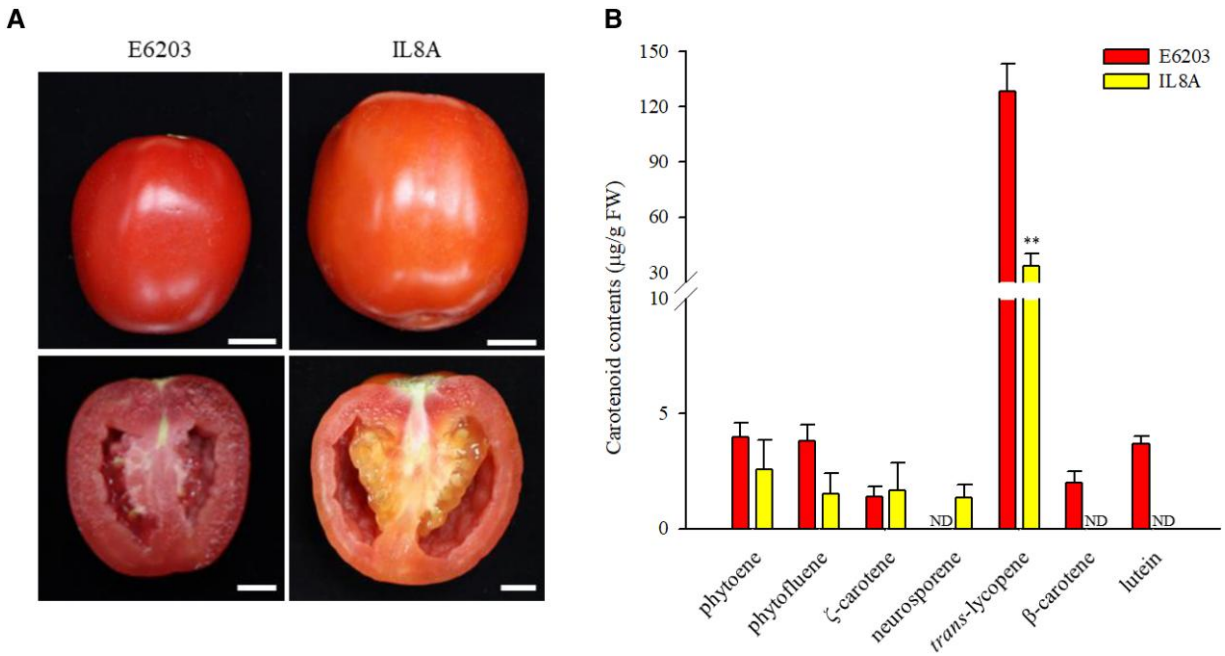

Figure 2 Fruit color and carotenoid variations in ripe fruit of E6203 and IL8A. A) Ripe fruit and B) carotenoid levels ($\mu g \cdot g^{-1}$ FW) in ripe fruit ($n = 5$) of E6203 and IL8A harvested at B + 10. Tomato plants were grown under the field conditions. The means of 5 replicates are shown with SE. ** indicates a significant difference at $P < 0.01$ according to an independent *t*-test. ND, not detected.

Downloaded from https://academic.oup.com/plphys/article/192/2/1289/7009207 by Biblioteca Centrale Agraria user on 16 June 2023

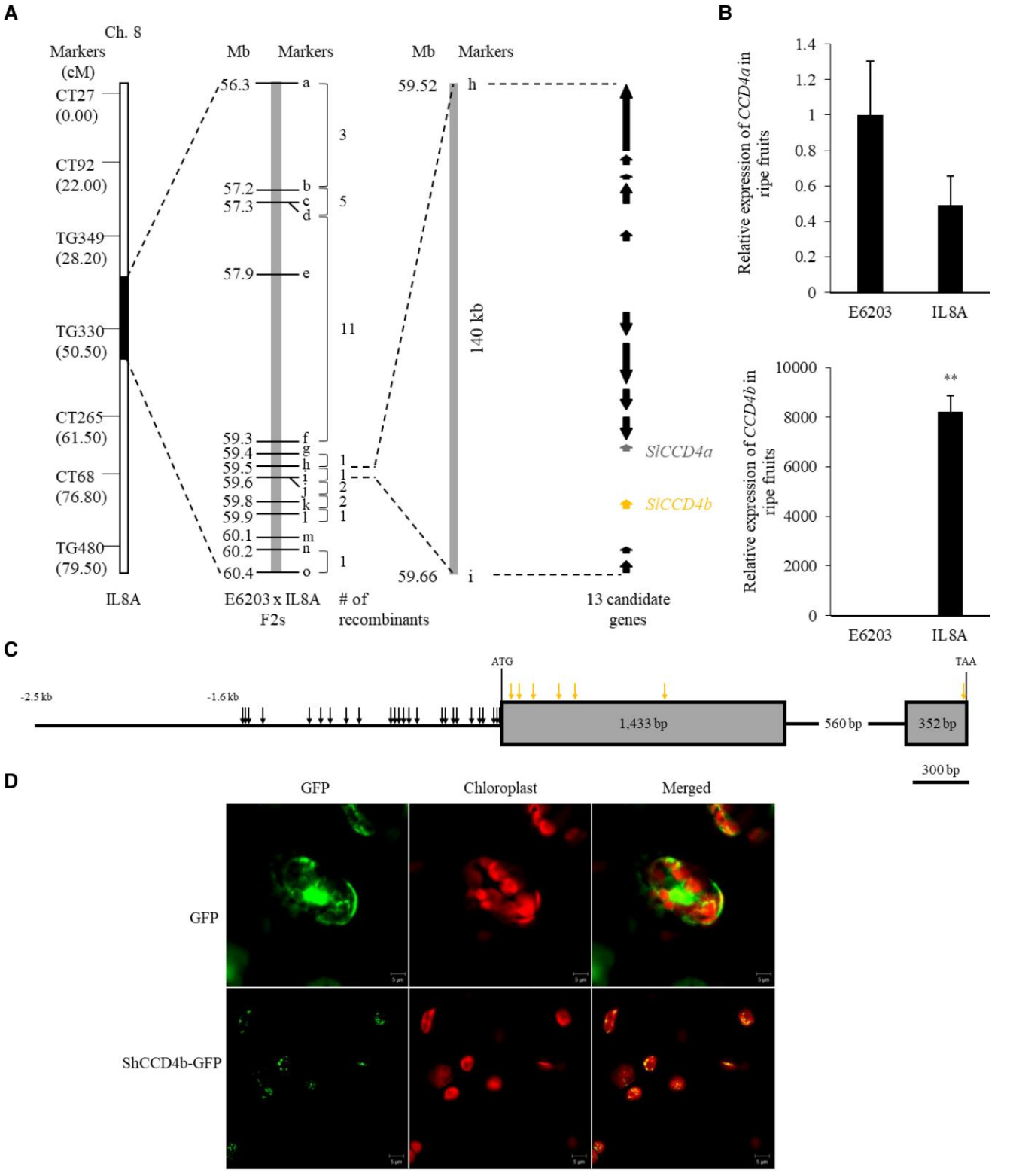

Figure 3 Positional cloning of genes regulating the dark orange color in IL8A and identification of *ShCCD4b*. A) Fine mapping of the dark orange color trait in IL8A. Arrows represent the predicted genes in the 140-kb candidate region on chromosome 8. B) Relative expression of *CCD4a* and *CCD4b* in ripe fruit ($n = 5$) of E6203 and IL8A. The means of 5 replicates are shown with SE. ** indicates a significant difference at $P < 0.01$ according to independent *t*-test. C) Seven nucleotide variations cause amino acid substitutions in ShCCD4b (red arrows), and 25 variations were located in the promoter region (black arrows). Arrows indicate the position for each variation. D) Co-expression of ShCCD4b-GFP was observed at the plastid. Scale bar = 5 μm.

Downloaded from https://academic.oup.com/plphys/article/192/2/1289/7009207 by Biblioteca Centrale Agraria user on 16 June 2023

(Supplemental Fig. S2) (Huang et al. 2009). The 7 amino acid changes were located in nonconserved regions of the CCD4 family. Amino acid variations at the DPMPK motif in tomato and grape (*Vitis vinifera*) were found. This motif is well conserved in most CCD4s and is proposed to restrict substrate penetration (Bruno et al. 2016). However, this motif was substituted to GPMPK in tomato CCD4b. In addition, VvCCD4a and VvCCD4b in grape were substituted to NPMPK and DPLPK, respectively (Lashbrooke et al. 2013).

To verify the predicted plastid transit peptide of ShCCD4b (Supplemental Fig. S2), the ShCCD4b-GFP fusion protein was transiently expressed in leaves of *Nicotiana benthamiana* under the control of the cauliflower mosaic virus (CaMV) 35S promoter. Agro-infiltrated leaves expressing pCAMBIA2300-ShCCD4b-eGFP were collected, and cellular localization of ShCCD4b was identified under confocal laser microscope. The GFP fluorescence signal at 488 nm showed that the ShCCD4b-GFP fusion protein was located inside the chloroplast, presumably in plastoglobules (Fig. 3D), compared with the control pCAMBIA2300-eGFP, which was distributed throughout the cytoplasm. CCD4 of Arabidopsis and *C. sativus* are localized in plastoglobules (Ytterberg et al. 2006, Rubio et al. 2008).

ShCCD4b-overexpressing tomatoes show distinct carotenoid profiles

To mimic the wild species allele and to investigate *ShCCD4b* function, *ShCCD4b*-overexpressing tomatoes were generated and carotenoids were analyzed in fruit, flowers, and leaves. Three independent transgenic tomato lines showed dark orange ripe fruit (Fig. 4A). Expression of *CCD4b* was greatly increased in ripe fruit of all transgenic lines, whereas expression of *CCD4a* was slightly increased in lines #4 and #10 (Fig. 4, B and C).

The carotenoid profiles were analyzed in B + 10 fruit of *ShCCD4b*-overexpressing plants over 3 generations (Table 1). Overall, the contents of phytoene, ζ-carotene, and neurosporene were increased, whereas *trans*-lycopene, β-carotene, and lutein contents were decreased in all

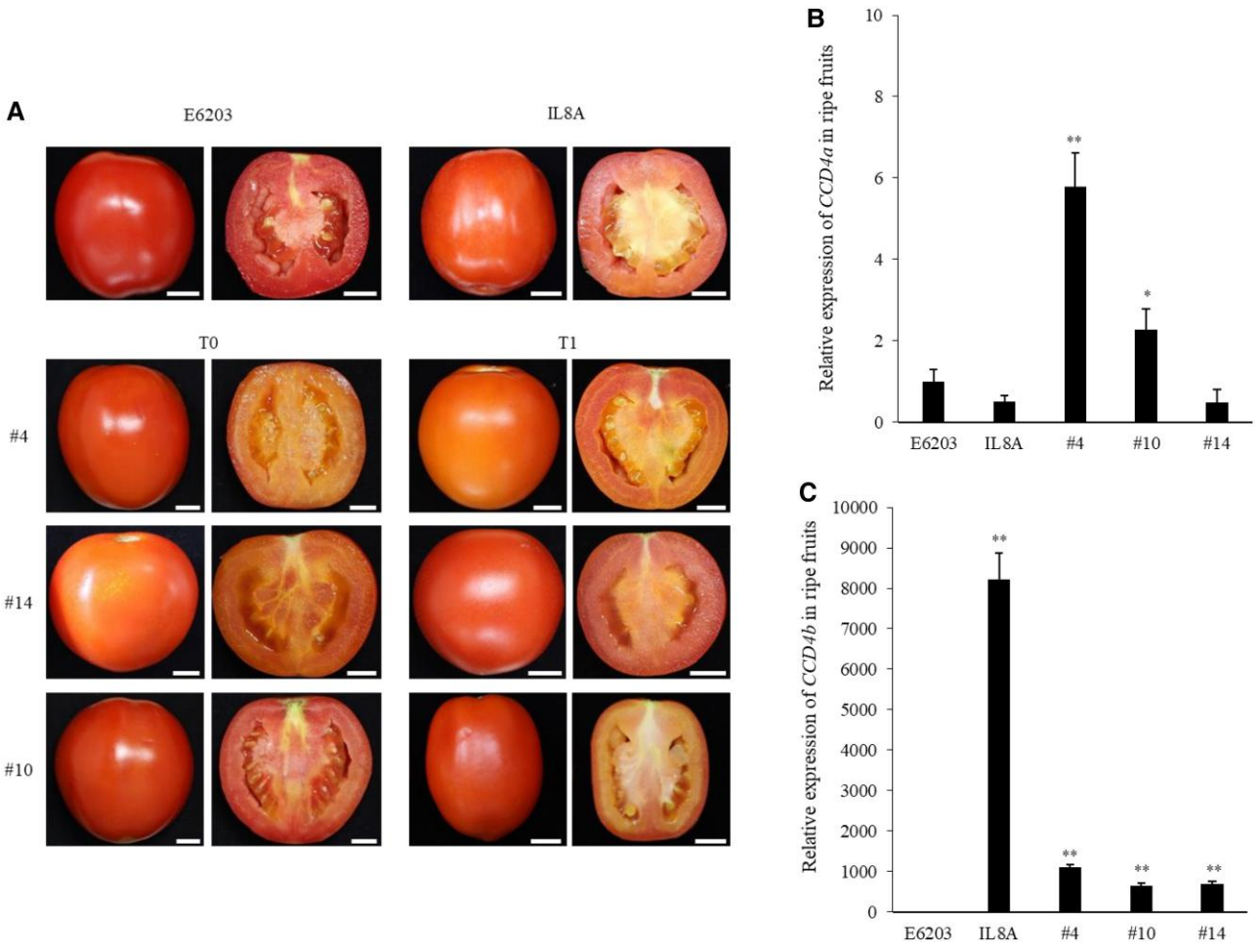

Figure 4 Ripe fruit harvested from *ShCCD4b*-overexpressing transgenic plants of the T_0 and T_1 generations, and expression analysis of *CCD4*s. A) Three independent lines, #4, #10, and #14, showed dark orange color in ripe fruit (B + 10). B) Relative expression of *CCD4a* and C) *CCD4b* in ripe fruit (B + 10) of the *ShCCD4b*-overexpressing tomatoes by RT-qPCR. The means of at least three replicates are shown with SE. * and ** indicate significant differences at $P < 0.05$ and $P < 0.01$, respectively, according to an independent *t*-test.

Downloaded from https://academic.oup.com/plphys/article/192/2/1289/7009207 by Biblioteca Centrale Agraria user on 16 June 2023

Table 1. Carotenoid contents in ripe fruit, flowers, and leaves of E6203, IL8A, and *ShCCD4b*-overexpressing lines (μg·g^{-1} FW, $n > 3$)

Ripe fruit		Phytoene	Phytofluene	ζ-carotene	Neurosporene	*trans*-lycopene	β-carotene	Lutein
T0	E6203	4.31 ± 0.48	3.69 ± 0.47	1.39 ± 0.57	ND	104.67 ± 16.43	2.41 ± 0.19	1.66 ± 0.08
	IL8A	1.63 ± 0.21	0.99 ± 0.12	0.74 ± 0.13	ND	33.41 ± 3.04**	0.58 ± 0.05**	0.28 ± 0.06**
	#4	16.36 ± 2.63**	9.49 ± 1.63**	19.70 ± 3.29**	0.87 ± 0.13**	56.50 ± 5.63*	ND	ND
	#10	4.47 ± 0.38	3.13 ± 0.31	2.70 ± 0.24	0.12 ± 0.02	88.86 ± 10.11	ND	0.27 ± 0.09**
	#14	14.69 ± 2.46**	7.98 ± 1.33**	15.39 ± 3.69**	0.96 ± 0.21**	49.92 ± 11.56**	ND	ND
T1	E6203	10.41 ± 2.22	7.49 ± 1.34	3.10 ± 1.12	ND	153.93 ± 10.07	3.99 ± 1.06	2.16 ± 0.40
	IL8A	5.52 ± 0.45	2.67 ± 0.35*	3.26 ± 0.80	0.08 ± 0.03	71.12 ± 4.66**	ND	ND
	#4–1	18.36 ± 3.88	10.12 ± 1.85	10.84 ± 1.87**	0.74 ± 0.20**	85.96 ± 10.01**	ND	ND
	#14–1	11.29 ± 2.48	6.57 ± 1.29	4.92 ± 1.39	0.45 ± 0.16**	73.62 ± 9.25**	ND	ND
T2	E6203	8.72 ± 1.27	6.53 ± 0.87	2.86 ± 0.38	ND	137.17 ± 6.91	1.83 ± 0.21	1.42 ± 0.10
	IL8A	14.10 ± 4.74	7.31 ± 2.36	12.23 ± 3.85*	0.03 ± 0.02**	68.20 ± 1.50**	ND	ND
	#4–1-17	15.41 ± 1.26	8.39 ± 0.75	17.57 ± 0.21**	0.12 ± 0.00**	50.31 ± 4.05**	ND	ND
	#10-8-25	12.85 ± 1.22	7.36 ± 0.72	10.28 ± 1.87*	0.07 ± 0.02**	84.51 ± 9.47**	ND	0.58 ± 0.02**
	#14-17-3	10.67 ± 0.83	5.60 ± 0.48	8.54 ± 0.74*	0.04 ± 0.00**	67.42 ± 9.25**	ND	ND

Flowers (T2)	Lutein	β-carotene	Zeaxanthin	Antheraxanthin	Violaxanthin	Neoxanthin
E6203	16.91 ± 1.50	6.25 ± 0.48	3.74 ± 0.30	59.73 ± 7.20	184.65 ± 18.41	84.70 ± 6.57
IL8A	9.49 ± 1.91*	3.43 ± 0.90	1.80 ± 0.39	35.07 ± 2.79	96.97 ± 5.16	58.25 ± 0.48
#4-1-17	9.61 ± 1.19*	3.98 ± 0.23	3.74 ± 0.20	42.04 ± 3.54	65.33 ± 2.90	30.77 ± 2.53
#10-8-25	13.26 ± 1.05	7.51 ± 1.75	2.89 ± 0.58	59.77 ± 12.46	134.15 ± 32.40	61.72 ± 15.68
#14-17-3	10.59 ± 0.88*	5.15 ± 0.98	3.06 ± 0.41	60.40 ± 14.17	81.98 ± 25.20	43.05 ± 18.39

Leaves (T2)	Lutein	β-carotene	Violaxanthin	Neoxanthin	Chlorophyll a	Chlorophyll b
E6203	295.91 ± 38.58	176.36 ± 26.86	48.17 ± 7.25	52.85 ± 9.20	18,318.31 ± 4983.60	12,547.68 ± 2148.14
IL8A	463.44 ± 63.24	252.79 ± 33.50	79.43 ± 10.29	55.09 ± 6.04	34,829.29 ± 4187.16	21,464.55 ± 2767.43
#4-1-17	330.24 ± 56.93	187.39 ± 31.82	55.15 ± 9.54	45.25 ± 7.42	24,473.12 ± 4708.66	14,662.86 ± 2540.15
#10-8-25	332.24 ± 36.64	182.58 ± 22.30	56.52 ± 6.76	42.67 ± 8.08	23,669.19 ± 3065.11	14,933.12 ± 1704.10
#14-17-3	430.07 ± 109.10	244.15 ± 58.57	72.71 ± 16.54	41.32 ± 10.04	32,541.43 ± 8451.21	20,265.22 ± 5399.23

ND, not detected. * and ** indicate significant differences at $P < 0.05$ and $P < 0.01$, respectively, according to Dunnett test. Data represents mean ± SE.

transgenic lines regardless of generation. Carotenoid profiles were consistent within all generations, indicating transgene phenotype heritability. Carotenoid level in IL8A was partly different from that in the overexpression lines. To dissect this, carotenoids of subIL8As were analyzed and a minor factor regulating the flux was found to reside in subIL8A-2, resulting in a slight reduction of some acyclic carotenoids (Supplemental Fig. S3 and Supplemental Table S3). The expression of isoprenoid and carotenoid biosynthetic genes in ripe fruit was not significantly altered in IL8A and transgenic lines (Supplemental Fig. S4), indicating that altered carotenoid profiles in IL8A and transgenic tomatoes was not caused by transcriptional regulation of isoprenoid and carotenoid biosynthetic genes. The carotenoid level in flowers was slightly decreased, and carotenoid and chlorophyll levels in leaves were not significantly altered in IL8A and transgenic lines (Table 1).

Volatile apocarotenoid analysis of ShCCD4b-overexpressing fruit

To identify cleaved products catalyzed by ShCCD4b, volatile apocarotenoids were analyzed in ripe fruit using solid-phase microextraction–gas chromatography–mass spectrometry (SPME-GC-MS) (Fig. 5A). The contents of MHO and citral were decreased in all transgenic fruit (T2 generation). Unlike the control, β-cyclocitral was not detected in IL8A and transgenic lines. Levels of geranylacetone and β-ionone were ∼2-fold higher in #4-1-17 and #14-17-3 fruit. α-Ionone was detected only in ripe fruit of #4-1-17 and #14-17-3. The increased apocarotenoids were derived from phytoene and ζ-carotene for geranylacetone, β-carotene for β-ionone, and δ-carotene and α-carotene for α-ionone by cleavage reactions at the C9–C10 (C9′–C10′) positions.

ShCCD4b cleaves β-carotene and ζ-carotene in E. coli

Escherichia coli strains engineered to produce carotenoids (Cunningham et al. 1993, Cunningham et al. 1994, Sun et al. 1996) were used to determine ShCCD4b activity. *ShCCD4b* expression was induced in the *E. coli* strains, producing phytoene, ζ-carotene, lycopene, δ-carotene, β-carotene, and zeaxanthin. Upon *ShCCD4b* expression, the color of the *E. coli* pellet was decreased in strains accumulating lycopene, δ-carotene, β-carotene, and zeaxanthin (Supplemental Fig. S5). Volatile apocarotenoids were analyzed using SPME-GC-MS in the *E. coli* cultures. Upon *ShCCD4b* expression, β-ionone was detected in the β-carotene-accumulating strain (Fig. 5B), and geranylacetone was detected in the ζ-carotene- and lycopene-accumulating strains (Fig. 5C). Apocarotenoid was not detected in phytoene-, δ-carotene-, and zeaxanthin-accumulating strains upon *ShCCD4b* expression. The precursors of geranylacetone are geranylgeranyl diphosphate, phytoene, and ζ-carotene, not lycopene (Vogel et al. 2008). In the lycopene-accumulating strain, ζ-carotene was detected

Downloaded from https://academic.oup.com/plphys/article/192/2/1289/7009207 by Biblioteca Centrale Agraria user on 16 June 2023

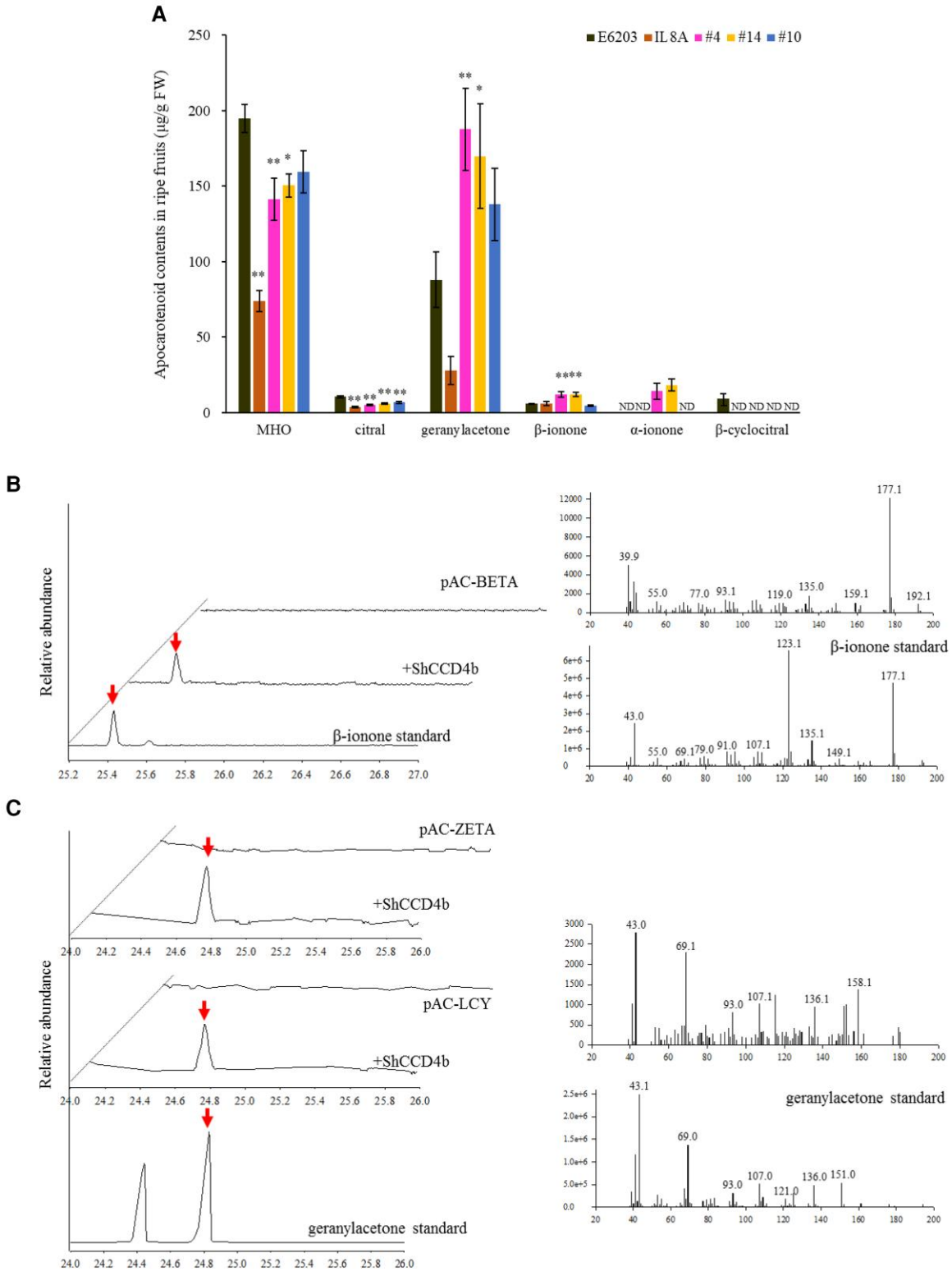

Figure 5 SPME-GC-MS analysis of ripe fruit and carotenoid-producing *e. coli*. A) Volatile apocarotenoid contents in ripe fruit of *ShCCD4b*-overexpressing plants by SPME-GC-MS analysis. The means of 3 replicates are shown with SE. * and ** indicate significant differences at $P < 0.05$ and $P < 0.01$, respectively, according to Dunnett test. ND, not detected. B) Chromatograms (left) obtained from SPME-GC-MS analyses of the control (top) and β-carotene-producing *E. coli* culture expressing *ShCCD4b* (middle) and β-ionone standard (bottom). The retention time and mass spectra (right) of the peak at 25.44 min from the *ShCCD4b*-expressing *E. coli* were identical to those of β-ionone. C) Chromatograms (left) obtained from SPME-GC-MS analysis of ζ-carotene (top) and lycopene-producing *E. coli* (middle) cultures and of geranylacetone standard (bottom). The mass spectra and retention time (right) of the peak at 24.78 min upon *ShCCD4b* expression showed identical fragmentation patterns with those of geranylacetone. Red arrows indicate the respective apocarotenoids upon *ShCCD4b* expression.

Downloaded from https://academic.oup.com/plphys/article/192/2/1289/7009207 by Biblioteca Centrale Agraria user on 16 June 2023

(Supplemental Table S4). Previously, geranylacetone was detected in the lycopene-accumulating strain upon *CCD1* expression, since ζ-carotene is a precursor of lycopene (Vogel et al. 2008). These data suggest that geranylacetone was generated from the cleavage reaction at the C9–C10 (C9′–C10′) positions of ζ-carotene. These results indicate that ShCCD4b catalyzes C9–C10 (C9′–C10′) cleavage to produce β-ionone from β-carotene and geranylacetone from ζ-carotene. Pseudoionone, generated from the cleavage reaction at the C9–C10 (C9′–C10′) positions of lycopene, were not detected in the lycopene-accumulating strain upon *ShCCD4b* expression (Supplemental Fig. S6), suggesting that *trans*-lycopene is not a substrate of ShCCD4b.

β-Cyclocitral-mediated control of fruit carotenoid synthesis

β-Cyclocitral treatment inhibited DXS activity and reduced metabolic flux in the methylerythritol phosphate (MEP) pathway in Arabidopsis (Mitra et al. 2021). Among the proposed ACSs (Hou et al. 2016), β-ionone, geranylacetone, and β-cyclocitral were differentially regulated in IL8A and transgenic fruit (Fig. 5). Hence, we examined the effect of the exogenous application of these apocarotenoids on ripening fruit. Exogenous β-cyclocitral (30 μM) fully blocked carotenoid synthesis, and 10 μM β-cyclocitral treatment significantly decreased carotenoid contents, except that of lutein, in ripening fruit of *S. lycopersicum* "M82', indicating its inhibitory effect on the pathway (Fig. 6). Exogenous beta-cyclocitral treatment of ripening fruit did not alter the expression of isoprenoid and carotenoid biosynthetic genes in a dose-dependent matter (Supplemental Fig. S7). Exogenous β-cyclocitral also inhibited carotenoid synthesis in a different tomato cultivar, Dafnis, as well as in bell pepper fruit (*Capsicum annuum*) (Supplemental Fig. S8; Supplemental Table S5). In Dafnis tomato, phytoene, phytofluene, and *trans*-lycopene levels were significantly decreased in a dose-dependent manner. The level of β-carotene was significantly decreased only with 20 μM β-cyclocitral treatment, and lutein levels were unaltered in M82 tomato. In bell peppers, all carotenoid levels were significantly decreased with both 15 and 20 μM β-cyclocitral treatment. Exogenous β-ionone and geranylacetone (20 μM) did not affect carotenoid synthesis in M82 ripening fruit (Supplemental Table S6). These results indicate that β-cyclocitral decreases carotenoid flux, presumably via inhibiting DXS activity as reported with β-cyclocitral-mediated inhibition of Arabidopsis DXS (Mitra et al. 2021).

Apocarotenoids control plant growth (Moreno et al. 2021); for example, exogenous β-cyclocitral increases root length in tomato, Arabidopsis, and rice (Dickinson et al. 2019). To identify the effect of *ShCCD4b* overexpression on plant development, plant height, length of lateral branches, number of lateral branches, and length of root were measured. Plant height, length of lateral branches, and the number of lateral branches were not significantly different at $P < 0.05$ and $P < 0.01$, respectively, according to Dunnett test in IL8A and transgenic lines compared with in E6203 (Supplemental Fig. S9). However, the root length at 6 d after germination was significantly decreased for both IL8A and transgenic plants compared with E6203 (Supplemental Fig. S10).

Discussion

Genetic nature of ShCCD4b

IL8A originating from *S. habrochaites* "LA1777' had dark orange fruit and reduced amounts of lycopene, β-carotene, and lutein (Fig. 2). Positional cloning using the F_2 populations derived from IL8A narrowed the genetic region of interest to a 140-kb region harboring only 13 genes (Fig. 3A). These

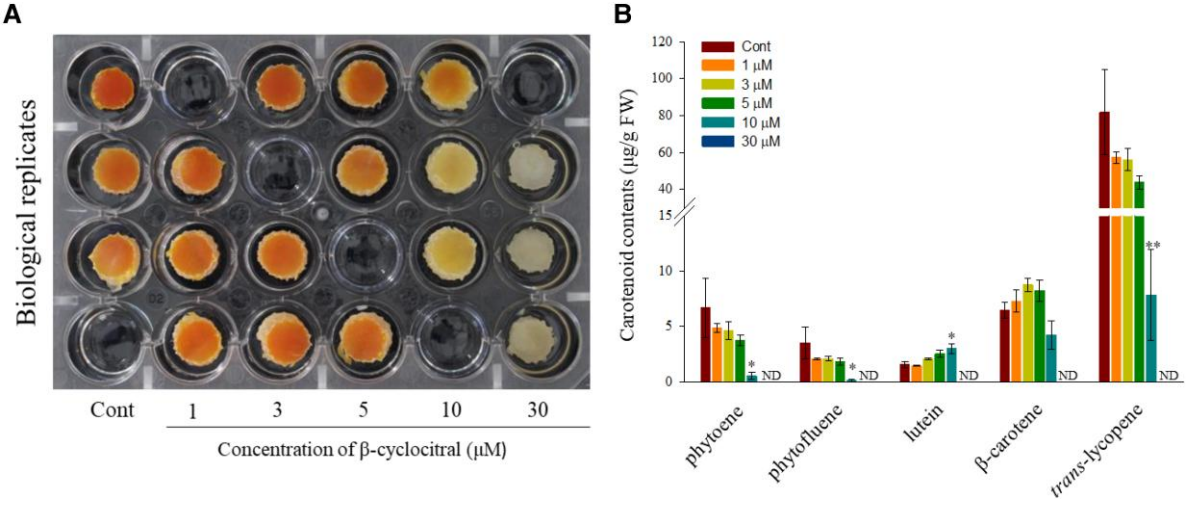

Figure 6 Reduced fruit pigmentation by exogenous β-cyclocitral in *s. lycopersicum* "M82'. A) Fruit disks ($n = 3$) from M82 plants at 10 d after treatment and B) carotenoid contents. The means are shown with SE. * and ** indicate significant differences at $P < 0.05$ and $P < 0.01$, respectively, according to Dunnett test. ND, not detected.

Downloaded from https://academic.oup.com/plphys/article/192/2/1289/7009207 by Biblioteca Centrale Agraria user on 16 June 2023

include 2 *CCD4*s, which are duplicate genes involved in carotenoid and apocarotenoid regulation in plants (Hou et al. 2016).

In tomato, 10 *CCD*s were found (Supplemental Fig. S11A), and *CCD1*, *CCD7*, and *CCD8* were identified. CCD1 is a major determinant of apocarotenoid production during fruit ripening and is responsible for cleaving multiple carotenoid substrates at the C9–C10 (C9′–C10′) positions. Reduced expression of *SlCCD1a* and *SlCCD1b* resulted in reduced levels of β-ionone and geranylacetone (Simkin et al. 2004). SlCCD7 regulates strigolactone biosynthesis, shoot branching, and arbuscular mycorrhiza-induced apocarotenoid production (Vogel et al. 2010b). SlCCD8 controls rhizosphere signaling and plant architecture via strigolactone biosynthesis (Kohlen et al. 2012).

*CCD4*s exist as duplicates in many species and often show developmental and environmental regulation of expression and substrate selectivity (Ohmiya et al. 2006, Ahrazem et al. 2010, Lashbrooke et al. 2013). Gene duplication can cause diversity or specificity in expression patterns or function (Duarte et al. 2006, Panchy et al. 2016). This divergent expression may result in functional diversity of duplicated genes by neo- and/or subfunctionalization, where functionality of ancestral genes is maintained because each duplicate has complementary differential subfunctions. Arabidopsis contains one copy of *CCD4* that is expressed in vegetative and floral tissues (Bruno et al. 2016). Duplicated *SlCCD4*s show specialized expression patterns, unlike *AtCCD4*. *SlCCD4b* is expressed in fruit, and its expression pattern is inversely associated with that of *SlCCD4a* (Supplemental Figure S11B), suggesting this duplication exhibits subfunctionalization and showing expression partitioning of *CCD4* in fruit.

The expression of *CCD4b* was greatly increased in ripe fruit of IL8A compared with in those of E6203 (Fig. 3B). Variations in the promoter region (~2.5 kb) (Fig. 3C) may cause the expression of quantitative trait loci of *CCD4b* in ripe fruit. Apocarotenoid abundance varies widely in ripe fruit of *S. habrochaites* "LA1777'; for example, β-ionone levels in LA1777 were 12-fold higher than those in the control (Mathieu et al. 2009). Our findings suggest that overexpression of *ShCCD4b* is the major determinant of the variations.

Carotenoid and apocarotenoid variations by ShCCD4b overexpression

Reduced levels of the major carotenoid *trans*-lycopene resulted in dark orange fruit in IL8A and transgenic lines (Fig. 4A), as *CCD4* is the genetic determinant of organ color in several crops (Ohmiya et al. 2006, Campbell et al. 2010, Rodrigo et al. 2013, Bai et al. 2015, Zhang et al. 2015). Due to overexpression of *ShCCD4b* in IL8A and transgenic tomatoes, phytoene, ζ-carotene, and neurosporene levels were increased, whereas *trans*-lycopene, β-carotene, and lutein levels were reduced (Table 1), although expression of isoprenoid and carotenoid biosynthetic genes was not significantly changed (Supplemental Fig. S4). These results indicate that the phenotypic variation is not due to transcriptional regulation of the endogenous biosynthetic genes. ShCCD4b cleaved ζ-carotene in *E. coli* but carotenoid profiles in tomato fruit (Table 1) were not associated with enzymatic activity (Fig. 5, B and C). However, the level of ζ-carotene increased in IL8A and transgenic lines.

In IL8A and transgenic lines, the changes in carotenoid levels in fruit were not observed in leaves or flowers (Table 1). The *SlCCD4b* expression in leaves was higher than that in flowers and *SlCCD4b* was not expressed in ripening fruit (Supplemental Fig. S11B). *SlCCD4b* may have enough endogenous expression in leaves and flowers, thus the *ShCCD4b* overexpression in leaves and flowers may not affect carotenoid composition unlike that in fruit. The major substrate of ShCCD4b is β-carotene, which is essential for photosynthesis, possibly implicating β-carotene stability under the cleavage attack in the leaves. Here, we propose 3 regulatory mechanisms through which *ShCCD4b* overexpression affects fruit carotenoids and apocarotenoids: (i) direct cleavage, (ii) precursor-dependent regulation, and (iii) apocarotenoid-mediated regulation. First, ShCCD4b directly cleaved ζ-carotene and β-carotene at C9–C10 (C9′–C10′), leading to increases in geranylacetone and β-ionone, respectively. Therefore, β-carotene deficiency by *ShCCD4b* overexpression is due in part to preferential substrate selectivity of ShCCD4b. This can also be due to precursor reduction. Second, the cleavage activity of ShCCD4b for catalyzing *trans*-lycopene was not identified in this study. ShCCD4b can cleave only at C9–C10 (C9′–C10′), whereas MHO and citral are derived from cleavage reactions at C5–C6 (C5′–C6′) and C7–C8 (C7′–C8′), respectively. Thus, reduced levels of MHO and citral may be in response to decreased lycopene levels. *trans*-lycopene was downregulated in IL8A and transgenic lines, even though *trans*-lycopene is not a substrate (Table 1). In the *tangerine* mutant, MHO level was significantly increased (Supplemental Table S7) (Vogel et al. 2010a), implying that CCDs prefer *cis*-configured lycopene as a substrate. Further analysis is necessary to determine a substrate preference of ShCCD4b. The lutein deficiency may be because of direct cleavage activity (Rodrigo et al. 2013) and reduced precursor levels. α-Carotene and lutein may act as ShCCD4b substrates, or only α-carotene may be catalyzed by ShCCD4b, leading to a lack of downstream lutein. δ-Carotene was not cleaved by ShCCD4b in vivo. Therefore, α-ionone, detected only in transgenic fruit, may be derived from α-carotene. Although cleavage of asymmetric carotenoid molecules by CCD4 is not very common, CCD4b1 from citrus preferentially cleaves the asymmetric carotenoids, α-carotene, and lutein. However, these cleavages only ocurr on the moiety containing the β-ionone ring (Rodrigo et al. 2013). Third, ζ-carotene level was elevated in transgenic plants even though ζ-carotene was directly cleaved by ShCCD4b, indicating that the increased level of the carotenoid flux may be higher than the turnover rate of geranylacetone from ζ-carotene by ACS.

Downloaded from https://academic.oup.com/plphys/article/192/2/1289/7009207 by Biblioteca Centrale Agraria user on 16 June 2023

Modern tomato varieties have poor fruit flavor. Improving flavor is one of the most important breeding goals (Tieman et al. 2017). Volatile apocarotenoids, including MHO, citral, geranylacetone, β-cyclocitral, and β-ionone, were mainly produced by CCD-dependent cleavage reactions from carotenoids (Vogel et al. 2010a). These volatile apocarotenoids were positively correlated with consumer liking and flavor intensity (Tieman et al. 2017). ShCCD4b catalyzes the cleavage reaction of ζ-carotene and β-carotene at the C9–C10 (C9′–C10′) double bond, increasing the abundance of geranylacetone and β-ionone, which are associated with preferred flavor (Fig. 5). β-Ionone was slightly increased (∼1.6-fold) in transgenic plants coupled with β-carotene deficiency. This may be partly in response to decreased flux to β-carotene by the cleavage of acyclic carotenoid(s). Small increases in apocarotenoid volatiles can be detected by consumers; for example, β-ionone has very low odor thresholds (0.007 nL/L) (Goff and Klee 2006).

ShCCD4b cleaves ζ-carotene and β-carotene

The CCD1 and CCD4 families show broad substrate specificity in plants. CCD4 typically produces β-ionone from cyclic carotenoids (Huang et al. 2009). Most CCD4s cleave only cyclic carotenoids at C9–C10 (C9′–C10′) (Rubio-Moraga et al. 2014, Bruno et al. 2015, Zhang et al. 2015, Bruno et al. 2016, Ahrazem et al. 2017). AtCCD4 does not cleave *cis*-ζ-carotene isomers in vivo and in vitro (Bruno et al. 2016). Uncommonly, VvCCD4a and VvCCD4b catalyze cleavage of acyclic carotenoids, lycopene, and neurosporene to produce MHO at C5–C6 (C5′–C6′) and geranylacetone at C9–C10 (C9′–C10′), respectively (Lashbrooke et al. 2013). VvCCD4b cleaves ζ-carotene at C9–C10 (C9′–C10′) to produce geranylacetone. In this study, ShCCD4b catalyzed the cleavage of acyclic carotenoid ζ-carotene and cyclic carotenoid β-carotene at C9–C10 (C9′–C10′) both in vivo and *in planta* (Fig. 5). Cleaving both acyclic and cyclic carotenoids is unusual for CCD4 (Huang et al. 2009, Bruno et al. 2016). Recently, structural and computational analyses of CCDs were conducted to propose putative functional residues (Daruwalla and Kiser 2020). A structural comparison study between VP14 and ZmCCD1 suggested that 3 key regions are important for determining substrate selectivity (Messing et al. 2010). The second region associated with accommodating the second ring of carotenoid in CCDs is E499PWPK503 residues (DPMPK motif) in VP14 (Messing et al. 2010). The conserved DPMPK motif is proposed to restrict substrate penetration (Bruno et al. 2016). This motif is well conserved in most CCD4s except SlCCD4s and VvCCD4s (Supplemental Fig. S2). Asp499 in AtCCD4 is substituted to Gly485 in SlCCD4b and ShCCD4b. Asp499 is substituted to Asn490 in VvCCD4a, and Met501 is substituted to Leu481 in VvCCD4b. These substitutions in the DPMPK motif could determine a substrate preference, appearing to select ζ-carotene as a substrate. Further analysis using the CCD4 variants will be necessary to find key residues for determining substrate specificity.

β-Cyclocitral inhibits carotenoid synthesis in fruit

The reduced level of total carotenoids in tomato fruit is considered to be a result of feedback regulation by β-carotene or one of its metabolites (Romer et al. 2000). In this study, the small molecule β-cyclocitral, derived from β-carotene, negatively controlled the carotenoid flux.

ShCCD4b cleaved β-carotene at C9–C10 (C9′–C10′) (Fig. 5B), leading to β-carotene deficiency (Table 1) and β-ionone upregulation (Fig. 5A). This cleavage process may induce the deficiency of β-cyclocitral derived from C7–C8 (C7′–C8′) cleavage due to precursor deficiency; subsequently, the carotenoid flux may be increased in *ShCCD4b*- overexpressing fruit (Table 1).

β-Cyclocitral levels in *old gold*, *yellow flesh*, and *tangerine* mutants (Supplemental Table S7), which have reduced levels of β-carotene, were significantly lower than in the near-isogenic control (Vogel et al. 2010a). β-Cyclocitral-treated pericarps of tomato and pepper showed decreased levels of carotenoids (Fig. 6). β-Cyclocitral binds to DXS and inhibits activity by blocking the active site in Arabidopsis (Mitra et al. 2021). DXS is a rate-limiting factor in the MEP pathway and a major determinant of carotenoid flux in plants (Estevez et al. 2001, Enfissi et al. 2005). Fruit-specific overexpression of DXS increased the carotenoid content in tomato (Enfissi et al. 2005). These results imply that β-cyclocitral deficiency in *ShCCD4b*-overexpressing fruit increases the carotenoid flux, presumably by increasing DXS activity. In addition, root length was decreased in IL8A and transgenic lines (Supplemental Fig. S10). Exogenous β-cyclocitral in tomatoes increased root length (Dickinson et al. 2019). These observations suggest that the metabolic and developmental alterations by *ShCCD4b* overexpression are mainly due to β-cyclocitral-mediated control (Fig. 7). Alternatively, β-cyclocitral could mediate a retrograde response of carotenoid-related gene expression. However, expression of the biosynthetic genes was not consistently altered in the *ShCCD4b*-overexpressing fruit (Supplemental Fig. S4) and β-cyclocitral-treated fruit (Supplemental Fig. S7). Generating specific ACSs by engineering CCD could improve carotenoid accumulation and resolve the regulatory mechanism of apocarotenoid signaling.

In this study, we identified natural overexpression of *CCD4* in tomato, controlling fruit color and flavor. In addition, a β-cyclocitral-derived regulatory mechanism was proposed to regulate carotenoid flux in tomato fruit. Enhancing volatiles that improve consumer liking is an emerging approach to ensure high fruit quality without negatively affecting yield-limiting sugar levels. Wild species have been well studied and exploited in mining for alleles to improve such volatile compounds (Klee and Tieman 2018). Identifying genetic determinants responsible for enhancing consumer-preferred apocarotenoids will facilitate breeding of new cultivars through marker-assisted selection.

Downloaded from https://academic.oup.com/plphys/article/192/2/1289/7009207 by Biblioteca Centrale Agraria user on 16 June 2023

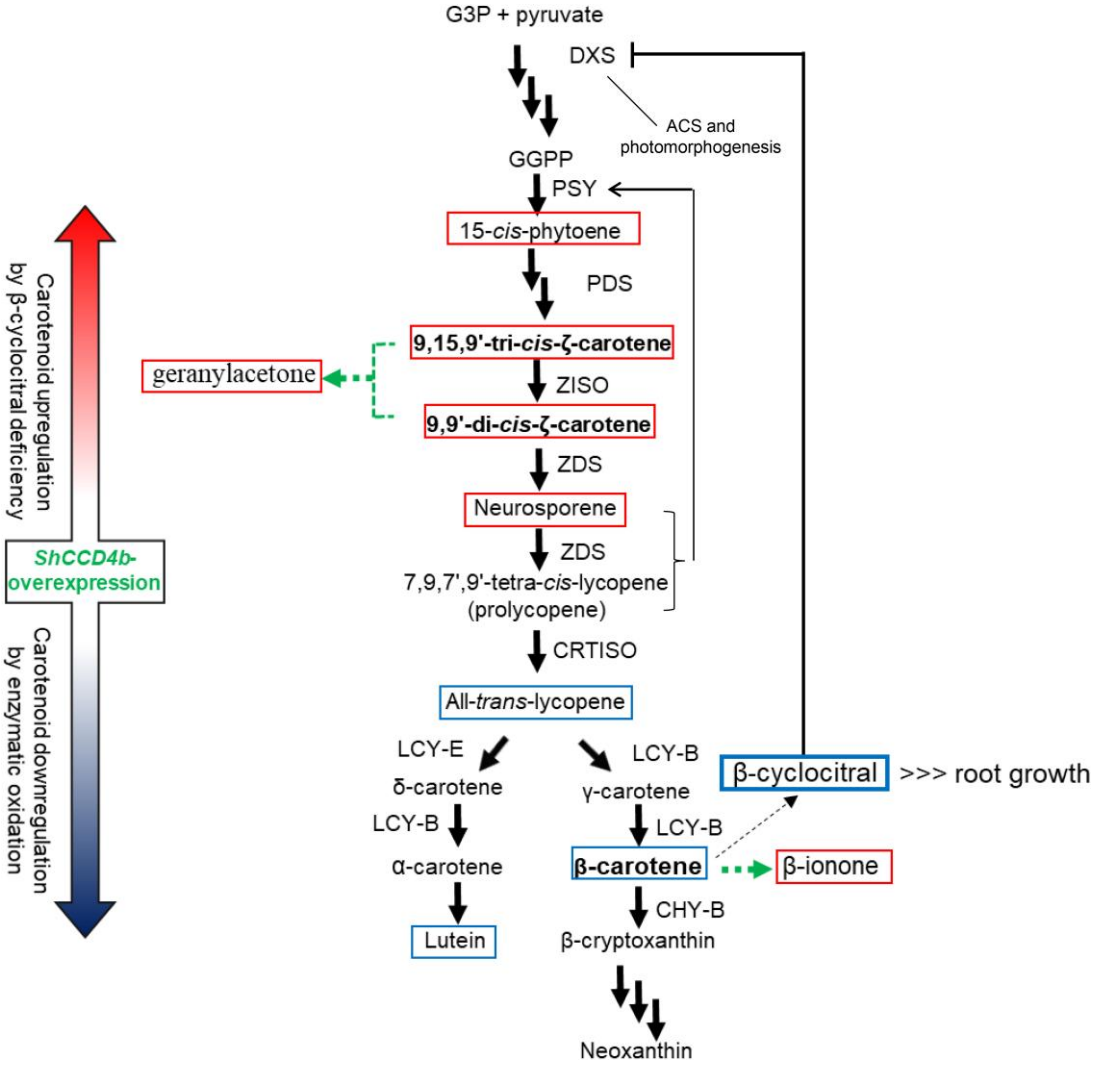

Figure 7 Working model of carotenoid and apocarotenoid regulation by *ShCCD4b* overexpression. ShCCD4b cleaves ζ-carotene and β-carotene at the C9–C10 (C9′–C10′) positions to generate geranylacetone and β-ionone, respectively. Endogenous deficiency and exogenous treatment of β-cyclocitral reveal β-carotene-dependent negative feedback regulation of carotenoid synthesis in tomato fruit (Romer et al. 2000). β-Cyclocitral inhibits DXS (Mitra et al. 2021), the rate-liming enzyme of the MEP pathway, and promotes root growth (Dickinson et al. 2019). A signal produced from prolycopene and/or neurosporene may upregulate the expression of *PSY1* (Kachanovsky et al. 2012). Apocarotenoid signal (ACS) and photomorphogenesis control plastid development and the expression of *DXS* in leaves (Cazzonelli et al. 2020). Black solid arrows and dashed arrows indicate the MEP/carotenoid and apocarotenoid pathways, respectively. Green dashed lines indicate the ShCCD4b-catalyzed apocarotenoid pathway. Bold carotenoids indicate substrates of ShCCD4b. The red box and blue box indicate upregulated and downregulated metabolites due to the *ShCCD4b* overexpression, respectively. G3P, D-glyceraldehyde 3-phosphate.

Materials and methods

Plant materials and growth conditions

'E6203' (*Solanum lycopersicum*) showing red fruit and IL8A (a *Solanum habrochaites* "LA1777' IL) showing dark orange fruit were used in this study (Fig. 2A). IL8A in the genetic background of the processing tomato cultivar E6203 belonged to a new set of Conserved Ortholog Set II-anchored ILs (S. Grandillo, unpublished data), which were developed to improve the previously published IL population (Monforte and Tanksley 2000). The mapping population was grown in the field of Cornell University, NY, USA, and other plants were grown under greenhouse conditions at Kyungpook National University (Daegu, Korea). Pericarps from ripe fruit were harvested at 10 d after breaker. Leaves from 10-week-old plants and open flowers were collected. All tissues were frozen in liquid nitrogen immediately after harvest and stored at −80°C until analysis.

To measure the parameters of shoot architecture, plants were grown for 4 wk in 128 trays (54 cm × 28 cm × 4 cm), 3 wk in 32 trays (54 cm × 28 cm × 5 cm), and 3 wk in pots (30 cm × 24.5 cm). Plant height, length of lateral branches, and the number of lateral branches were measured in 10-week-old plants. To measure the root length, plants

Downloaded from https://academic.oup.com/plphys/article/192/2/1289/7009207 by Biblioteca Centrale Agraria user on 16 June 2023

were sown in petri dishes. Six days after germination, root length was measured ($n > 13$).

Accession numbers

Accession numbers are shown in Supplemental Fig. S2, Supplemental Fig. S11, and Supplemental Table S8.

Genetic mapping

A total of 216 F_2 plants derived from a cross between E6203 and IL8A were used to identify genes controlling fruit color in IL8A. Genomic DNA from young leaves was extracted using the CTAB method (Murray and Thompson 1980). Primers used for genetic mapping are listed in Supplemental Table S1. Previously developed markers, C2_At5g11490 (marker c) and C2_At4g19003 (marker m), were used to identify introgressed segments of the *S. habrochaites* "LA1777' chromosome. Furthermore, an additional 11 makers were developed using expressed sequence tags of *S. habrochaites* (Dai et al. 2010).

RNA isolation and gene expression analysis

Total RNA was isolated from leaves and open flowers using TRI REAGENT (Molecular research center, Ohio, USA) and from fruit using Ribospin™ Seed/Fruit (GeneAll, Korea). Gene expression was analyzed via RT-qPCR. Total RNA (1 μg) was reverse-transcribed to synthesize first-strand cDNA using a DiaStar™ RT-kit (Solgent, Korea), following the manufacturer's instructions, with an 18-bp oligo dT primer. RT-qPCR was conducted using SYBR qPCR Master Mix (Applied Biosystems, USA), according to the manufacturer's instructions, with gene-specific primers (Supplemental Table S8) and 100 ng cDNA in a 10-μl final volume. At least 3 biological replicates and 2 technical replications were performed per primer. Actin was used as a reference gene to normalize gene expression (Powell et al. 2012). RT-qPCR was conducted with an initial denaturation at 95°C for 10 min, then 40 subsequent cycles of denaturation at 95°C for 15 s, with annealing and extension at 60°C for 1 min. RT-qPCR was performed on a StepOneplus™ Thermal Cycler (Applied Biosystems, USA) and analyzed using StepOne software v2.0 (Applied Biosystems, USA). Following the reactions, specificity of the PCR amplification was assessed by the presence of a single peak in the melt curve performed after the amplification steps.

Subcellular localization of ShCCD4b

The full-length *ShCCD4b*—without the stop codon—was amplified using specific primers (Supplemental Table S1) and fused with the *GFP* gene in pCAMBIA2300:eGFP to construct the plasmid ShCCD4b:eGFP under the control of the CaMV 35S promoter. Amplified ShCCD4b and pCAMBIA2300:eGFP were digested with *Xba*I and *Sal*I and inserted into the compatible *Xba*I and *Sal*I site of pCAMBIA2300:eGFP using T4 DNA ligase (Promega Corporation, USA). The resultant plasmid ShCCD4b:eGFP was transformed into *E. coli* DH5α and sequenced (Solgent, Korea). The recombinant ShCCD4b:eGFP vector was then transferred into *Agrobacterium tumefaciens* GV3101 using the freeze–thaw method (Chen et al. 1994).

Agrobacterium cultures were grown at 28°C until reaching an OD_{600} of 0.7, resuspended in an induction buffer (10 mM MES, 10 mM $MgCl_2$, 200 μM acetosyringone), and then incubated at room temperature for 2 h before agroinfiltration (Ma et al. 2013, Frusciante et al. 2014). Young leaves of 6-week-old *Nicotiana benthamiana* plants were agroinfiltrated with GV3101 containing either pCAMBIA2300:eGFP or ShCCD4b:eGFP. After 2 d, leaves were analyzed using confocal laser-scanning microscopy (LSM700, Carl Zeiss, Oberkochen, Germany). Chloroplasts were identified via their autofluorescence at 555 nm with red fluorescence, and GFP was identified at 488 nm with green fluorescence.

Generation of ShCCD4b-overexpressing tomatoes

The full-length *ShCCD4b* sequence was cloned using the pCAMBIA2300-LIC vector containing the CaMV 35S promoter. To amplify the *ShCCD4b* coding region, specific primers were designed including adaptor sequences for the ligation independent cloning (LIC) method (Supplemental Table S1). Amplified PCR products were treated with T4 polymerase and dATP at 22°C for 30 min, and then T4 polymerase was inactivated at 75°C for 20 min. pCAMBIA2300-LIC was digested with *Pst*I and treated with T4 polymerase and dTTP. T4 polymerase-treated PCR product was mixed with T4 polymerase-treated pCAMBIA2300-LIC at room temperature for 60 min through the LIC method. The mixture was then transformed into *E. coli* DH5α. The resulting plasmid vector was introduced into *Agrobacterium tumefaciens* LBA4404 and transformed into E6203 using previously described methods (Fillatti et al. 1987). Plants that inherited the transgene were identified by PCR using a specific primer, CCD4-OX-4 (Supplemental Table S1). T0 and T1 generations were grown in peat-based compost supplemented with fertilizer, and T2 generation was grown in rock wool media connected to an automatic irrigation system as previously described (Yoo et al. 2019).

CCD4 activity assay

The carotenoid-accumulating *E. coli* strains were used to perform the functional complementation assays. The cDNA of *ShCCD4b* lacking the putative plastid transit peptide sequence was amplified using specific primers (Supplemental Table S1), and PCR products were cloned into pTcrHis2-TOPO vectors (Invitrogen, USA). The recombinant clones were cotransformed into *E. coli* strains engineered to produce phytoene (pAC-PHYT), ζ-carotene (pAC-ZETA), lycopene (pAC-LYC), δ-carotene (pAC-DELTA), β-carotene (pAC-BETA), and zeaxanthin (pAC-ZEAX) (Cunningham et al. 1993, Cunningham et al. 1994, Sun et al. 1996).

For carotenoid analysis, colonies of transformed *E. coli* were cultured overnight at 37°C in 5 ml LB medium containing appropriate antibiotics: 34 μg/ml chloramphenicol and

Downloaded from https://academic.oup.com/plphys/article/192/2/1289/7009207 by Biblioteca Centrale Agraria user on 16 June 2023

100 μg/ml ampicillin. The cultured cells were transferred to 100 ml LB medium supplemented with antibiotics (Ahrazem et al. 2016b). Then, the cultures were incubated at 37°C with gentle shaking (125 rpm) until reaching an OD_{600} of 0.6. After adding 0.2 mM isopropyl-β-D-thiogalactopyranoside (IPTG), the *ShCCD4b*-expressing strains were grown at 28°C for an additional 12 h and gently shaken (125 rpm). The *E. coli* cells were harvested by centrifugation at 4°C and 4000 rpm for 10 min. Harvested cells were transferred to 2-ml screw cap tubes, with 2 6-mm glass beads, and stored at −80°C.

To analyze volatile apocarotenoids, colonies of transformed *E. coli* were cultured overnight at 37°C in 0.5 ml LB medium supplemented with antibiotics. The cultured cells were transferred to 20 ml LB medium containing appropriate antibiotics in 250-ml flasks and incubated at 37°C with gentle shaking (125 rpm) until the OD_{600} reached 0.6. The cell cultures (5 ml) were transferred to tightly closed 10-ml vials, and then 0.2 mM IPTG was added to the *ShCCD4b*-expressing strains. The vials were incubated at 16°C for 12 h, and then 2.5 ml 100 mM EDTA (pH 7.5) and 5.5 g $CaCl_2{\cdot}2H_2O$ were added and sonicated for 5 min. The headspace volatiles were immediately adsorbed by the SPME fiber—65 μm polydimethylsiloxane-divinylbenzene (PDMS/DVB, Supelco Inc., Bellefonte, PA, USA)—through a septum and then analyzed by GC-MS (7890B-5977B GC/MSD, Agilent, Santa Clara, CA, USA).

Carotenoid and apocarotenoid analysis

Carotenoids and chlorophylls were extracted from ripe fruit (B + 10), flowers, leaves (10 weeks old), and bacterial cultures producing carotenoids (Yoo et al. 2017). In floral tissues, saponification was conducted after carotenoid extraction (Kim et al. 2017).

Apocarotenoid volatile extraction and analysis were conducted as previously described (Rambla et al. 2017, Yoo et al. 2019). For ripe fruit, 3 g sliced pericarp was collected in a 10-ml SPME vial and incubated at 37°C for 10 min. Then, 3 ml 100 mM EDTA (pH 7.5) and 6.6 g $CaCl_2{\cdot}2H_2O$ were added for 5 min of sonication. To analyze volatile apocarotenoids in the bacterial headspace, 2.5 ml 100 mM EDTA (pH 7.5) and 5.5 g $CaCl_2{\cdot}2H_2O$ were added with 5 min of sonication. Volatile extracts were analyzed within 12 h. Samples in the 10-ml SPME vial were incubated for 30 min at 50°C. The 65-μm PDMS/DVB fiber (Supelco Inc., Bellefonte, PA, USA) was exposed to the vial headspace for 30 min at 50°C. Volatile analysis was conducted on a GC-MS at the Kyungpook National University Instrumental Analysis Center (Daegu, Korea). The volatiles were desorbed in the injection port of the gas chromatograph for 1 min at 250°C in splitless mode. Separation was performed on a DB-5 ms column (60 m × 0.25 mm, 1-μm film thickness; J&W Scientific, Folsom, CA, USA). Helium was used as the carrier gas at a flow rate of 1.2 ml min^{-1}. The temperature program was started at 35°C for 2 min, followed by a 5°C min^{-1} ramp to 250°C, with a 5-min hold at 250°C. Mass spectra were obtained at an ionization energy of 70 eV and a scan speed of 7 scans/s^{-1} with a mass-to-charge ratio scan range of 35 to 220. Agilent MassHunter software (version B.02.17, Santa Clara, CA, USA) was used for data analysis. Compounds were identified by comparing the GC retention time and mass spectra using the mass spectral library of the Wiley Registry (11th Edition/NIST 2017).

Apocarotenoid treatment in ripening fruit

Fruit at breaker stage were harvested from 2 tomato cultivars (M82 and Dafnis) and bell pepper (*Capsicum annuum* "Sirocco') and treated with β-cyclocitral (Sigma-Aldrich, St. Louis, MO, USA), β-ionone (Sigma-Aldrich, St. Louis, MO, USA), and geranylacetone (Tokyo Chemical Industry Co., Ltd., Japan), as previously described (Pankratov et al. 2016). Disks collected from the same fruit were placed epidermis side down in individual wells of 24-well tissue culture plates (SPL Life Sciences, Pocheon, Korea). Stock solution of 10-mM β-cyclocitral was prepared in DMSO, and 10 mM β-ionone and geranylacetone were prepared in ethanol. Apocarotenoids and the control solutions (10 mM Tris–HCl (pH 8.5) containing DMSO or ethanol) were applied (150 μl) on top of the explant. The plates were incubated at 25°C with a light/dark cycle of 16 h/8 h. To achieve high humidity during incubation, empty wells in each plate were filled with sterile water. The fruit disks at 10 d after the treatment were analyzed for carotenoids.

Statistical analysis

Statistical analysis was conducted using SPSS 25 software (IBM, Armonk, New York, USA). Independent *t*-tests and Dunnett tests were employed to determine significant differences at levels of 5% and 1%.

Author contributions

J.M.L., H.J.Y., and J.J.G. designed the research. H.J.Y., M.Y.C., H.A.L., S.B.L., and J.M.L. performed the experiments and analyzed the data. S.G. and J.J.G. provided experimental resources. H.J.Y. and J.M.L. analyzed the data and wrote the manuscript.

Supplemental data

The following materials are available in the online version of this article.

Supplemental Table S1. Primers used in this study.

Supplemental Table S2. Candidate genes spanning the 140-kb region on chromosome 8.

Supplemental Table S3. Carotenoid contents in subIL8As, IL8A, and E6203 (μg·g-1 FW, $n = 5$).

Supplemental Table S4. Carotenoid contents in *ShCCD4b*-expresssing *E. coli* strains engineered to produce different carotenoid (μg·g-1, $n = 3$).

Downloaded from https://academic.oup.com/plphys/article/192/2/1289/7009207 by Biblioteca Centrale Agraria user on 16 June 2023

Supplemental Table S5. Carotenoid contents in tomato and bell pepper fruit at 10 d after β-cyclocitral treatment ($\mu g \cdot g^{-1}$ FW, $n > 3$).

Supplemental Table S6. Carotenoid contents in M82 fruit at 10 d after β-ionone and geranylacetone treatment ($\mu g \cdot g^{-1}$ FW, $n = 3$).

Supplemental Table S7. Volatile apocarotenoid contents in ripe fruit of Alisa Craig and LA3183 (*tangerine*) (μg·g-1 FW, $n = 3$).

Supplemental Table S8. Primers used for RT-qPCR.

Supplemental Fig. S1. Relative expression of candidate genes in ripe fruit, flowers, and leaves of E6203 and IL8A ($n > 3$) by RT-qPCR.

Supplemental Fig. S2. Alignment of amino acid sequences of CCDs of various plants.

Supplemental Fig. S3. SubIL map for dissecting IL8A.

Supplemental Fig. S4. Relative expression of isoprenoid and carotenoid biosynthetic genes in ripe fruit of T0 and T1 generations ($n > 3$, B + 10) by RT-qPCR.

Supplemental Fig. S5. Expression of *ShCCD4b* in *E. coli* strains producing different carotenoids.

Supplemental Fig. S6. SPME-GC-MS analysis of lycopene-producing *E. coli*.

Supplemental Fig. S7. Relative expression of isoprenoid and carotenoid biosynthetic genes in β-cyclocitral-treated M82 fruit ($n > 3$) by RT-qPCR.

Supplemental Fig. S8. Reduced pigmentation (upper) and relative expression of *DXS* (lower) by exogenous β-cyclocitral in tomato (*S. lycopersicum* "Dafnis') and bell pepper (*C. annuum* "Sirocco') fruit at 10 d after treatment.

Supplemental Fig. S9. Measurement of plant growth parameters in *ShCCD4b*-overexpressing tomatoes.

Supplemental Fig. S10. Reduced root length in *ShCCD4b*-overexpressing tomatoes.

Supplemental Fig. S11. CCD family in tomato.

Funding

This work was supported by the National Research Foundation of Korea grant funded by the Korea government (MSIT) (2021R1A2C2093789).

Conflict of interest statement. None declared.

References

Ahrazem O, Diretto G, Argandona J, Rubio-Moraga A, Julve JM, Orzaez D, Granell A, Gomez-Gomez L. Evolutionarily distinct carotenoid cleavage dioxygenases are responsible for crocetin production in Buddleja davidii. J Exp Bot. 2017:**68**(16): 4663–4677. https://doi.org/10.1093/jxb/erx277

Ahrazem O, Gomez-Gomez L, Rodrigo MJ, Avalos J, Limon MC. Carotenoid cleavage oxygenases from microbes and photosynthetic organisms: features and functions. Int J Mol Sci. 2016a:**17**(11): e1781. https://doi.org/10.3390/ijms17111781

Ahrazem O, Rubio-Moraga A, Berman J, Capell T, Christou P, Zhu C, Gomez-Gomez L. The carotenoid cleavage dioxygenase CCD2 catalysing the synthesis of crocetin in spring crocuses and saffron is a plastidial enzyme. New Phytol. 2016b:**209**(2): 650–663. https://doi.org/10.1111/nph.13609

Ahrazem O, Trapero A, Gomez MD, Rubio-Moraga A, Gomez-Gomez L. Genomic analysis and gene structure of the plant carotenoid dioxygenase 4 family: a deeper study in Crocus sativus and its allies. Genomics. 2010:**96**(4): 239–250. https://doi.org/10.1016/j.ygeno.2010.07.003

Alder A, Jamil M, Marzorati M, Bruno M, Vermathen M, Bigler P, Ghisla S, Bouwmeester H, Beyer P, Al-Babili S. The path from beta-carotene to carlactone, a strigolactone-like plant hormone. Science. 2012:**335**(6074): 1348–1351. https://doi.org/10.1126/science.1218094

Ansari M, Emami S. beta-Ionone and its analogs as promising anticancer agents. Eur J Med Chem. 2016:**123**: 141–154. https://doi.org/10.1016/j.ejmech.2016.07.037

Avendano-Vazquez AO, Cordoba E, Llamas E, San Roman C, Nisar N, De La Torre S, Ramos-Vega M, Gutierrez-Nava MD, Cazzonelli CI, Pogson BJ, et al. An uncharacterized apocarotenoid-derived signal generated in zeta-carotene desaturase mutants regulates leaf development and the expression of chloroplast and nuclear genes in Arabidopsis. Plant Cell. 2014:**26**(6): 2524–2537. https://doi.org/10.1105/tpc.114.123349

Bai S, Tuan PA, Tatsuki M, Yaegaki H, Ohmiya A, Yamamizo C, Moriguchi T. Knockdown of carotenoid cleavage dioxygenase 4 (CCD4) via virus-induced gene silencing confers yellow coloration in peach fruit: evaluation of gene function related to fruit traits. Plant Mol Biol Rep. 2015:**34**(1): 257–264. https://doi.org/10.1007/s11105-015-0920-8

Bruno M, Beyer P, Al-Babili S. The potato carotenoid cleavage dioxygenase 4 catalyzes a single cleavage of beta-ionone ring-containing carotenes and non-epoxidated xanthophylls. Arch Biochem Biophys. 2015:**572**: 126–133. https://doi.org/10.1016/j.abb.2015.02.011

Bruno M, Koschmieder J, Wuest F, Schaub P, Fehling-Kaschek M, Timmer J, Beyer P, Al-Babili S. Enzymatic study on AtCCD4 and AtCCD7 and their potential to form acyclic regulatory metabolites. J Exp Bot. 2016:**67**(21): 5993–6005. https://doi.org/10.1093/jxb/erw356

Campbell R, Ducreux LJ, Morris WL, Morris JA, Suttle JC, Ramsay G, Bryan GJ, Hedley PE, Taylor MA. The metabolic and developmental roles of carotenoid cleavage dioxygenase4 from potato. Plant Physiol. 2010:**154**(2): 656–664. https://doi.org/10.1104/pp.110.158733

Cazzonelli CI, Hou X, Alagoz Y, Rivers J, Dhami N, Lee J, Marri S, Pogson BJ. A cis-carotene derived apocarotenoid regulates etioplast and chloroplast development. Elife. 2020:**9**: e45310. https://doi.org/10.7554/eLife.45310

Chen H, Nelson RS, Sherwood JL. Enhanced recovery of transformants of Agrobacterium tumefaciens after freeze-thaw transformation and drug selection. Biotechniques. 1994:**16**(4): 664–668, 670.

Chetelat RT, Meglic V. Molecular mapping of chromosome segments introgressed from Solanum lycopersicoides into cultivated tomato (Lycopersicon esculentum). Theor Appl Genet. 2000:**100**(2): 232–241. https://doi.org/10.1007/s001220050031

Cunningham FX, Chamovitz D, Misawa N, Gantt E, Hirschberg J. Cloning and functional expression inEscherichia coliof a cyanobacterial gene for lycopene cyclase, the enzyme that catalyzes the biosynthesis of β-carotene. FEBS Lett. 1993:**328**(1–2): 130–138. https://doi.org/10.1016/0014-5793(93)80980-9

Cunningham FX J, Sun Z, Chamovitz D, Hirschberg J, Gantt E. Molecular structure and enzymatic function of lycopene cyclase from the cyanobacterium Synechococcus sp strain PCC7942. Plant Cell. 1994:**6**(8): 1107–1121. https://doi: 10.1105/tpc.6.8.1107

Dai X, Wang G, Yang DS, Tang Y, Broun P, Marks MD, Sumner LW, Dixon RA, Zhao PX. TrichOME: a comparative omics database for plant trichomes. Plant Physiol. 2010:**152**(1): 44–54. https://doi.org/10.1104/pp.109.145813

Downloaded from https://academic.oup.com/plphys/article/192/2/1289/7009207 by Biblioteca Centrale Agraria user on 16 June 2023

D'alessandro S, Ksas B, Havaux M. Decoding beta-cyclocitral-mediated retrograde signaling reveals the role of a detoxification response in plant tolerance to photooxidative stress. Plant Cell. 2018:**30**(10): 2495–2511. https://doi.org/10.1105/tpc.18.00578

Daruwalla A, Kiser PD. Structural and mechanistic aspects of carotenoid cleavage dioxygenases (CCDs). Biochim Biophys Acta Mol Cell Biol Lipids. 2020:**1865**(11): 158590. https://doi.org/10.1016/j.bbalip.2019.158590

Dickinson AJ, Lehner K, Mi J, Jia KP, Mijar M, Dinneny J, Al-Babili S, Benfey PN. beta-Cyclocitral is a conserved root growth regulator. Proc Natl Acad Sci U S A. 2019:**116**(21): 10563–10567. https://doi.org/10.1073/pnas.1821445116

Dickinson AJ, Zhang J, Luciano M, Wachsman G, Schnermann M, Dinneny J, Benfey PN. A plant lipocalin promotes retinal-mediated oscillatory lateral root initiation. Science. 2021:**373**(6562): 1532–1536. https://doi.org/10.1126/science.abf7461

Diretto G, Frusciante S, Fabbri C, Schauer N, Busta L, Wang Z, Matas AJ, Fiore A JKCR, Fernie AR, Jetter R, et al. Manipulation of beta-carotene levels in tomato fruits results in increased ABA content and extended shelf life. Plant Biotechnol J. 2020:**18**(5): 1185–1199. https://doi.org/10.1111/pbi.13283

Duarte JM, Cui L, Wall PK, Zhang Q, Zhang X, Leebens-Mack J, Ma H, Altman N, Depamphilis CW. Expression pattern shifts following duplication indicative of subfunctionalization and neofunctionalization in regulatory genes of Arabidopsis. Mol Biol Evol. 2006:**23**(2): 469–478. https://doi.org/10.1093/molbev/msj051

Dun EA, Brewer PB, Beveridge CA. Strigolactones: discovery of the elusive shoot branching hormone. Trends Plant Sci. 2009:**14**(7): 364–372. https://doi.org/10.1016/j.tplants.2009.04.003

Enfissi EM, Fraser PD, Lois LM, Boronat A, Schuch W, Bramley PM. Metabolic engineering of the mevalonate and non-mevalonate isopentenyl diphosphate-forming pathways for the production of health-promoting isoprenoids in tomato. Plant Biotechnol J. 2005:**3**(1): 17–27. https://doi.org/10.1111/j.1467-7652.2004.00091.x

Eshed Y, Zamir D. An introgression line population of Lycopersicon pennellii in the cultivated tomato enables the identification and fine mapping of yield-associated QTL. Genetics. 1995:**141**(3): 1147–1162. https://doi.org/10.1093/genetics/141.3.1147

Estevez JM, Cantero A, Reindl A, Reichler S, Leon P. 1-Deoxy-D-xylulose-5-phosphate Synthase, a limiting enzyme for plastidic isoprenoid biosynthesis in plants. J Biol Chem. 2001:**276**(25): 22901–22909. https://doi.org/10.1074/jbc.M100854200

Fan P, Leong BJ, Last RL. Tip of the trichome: evolution of acylsugar metabolic diversity in Solanaceae. Curr Opin Plant Biol. 2019:**49**: 8–16. https://doi.org/10.1016/j.pbi.2019.03.005

Fillatti JJ, Kiser J, Rose R, Comai L. Efficient transfer of a glyphosate tolerance gene into tomato using a binary Agrobacterium Tumefaciens vector. Nat Biotechnol. 1987:**5**(7): 726–730. https://doi.org/10.1038/nbt0787-726

Frusciante S, Diretto G, Bruno M, Ferrante P, Pietrella M, Prado-Cabrero A, Rubio-Moraga A, Beyer P, Gomez-Gomez L, Al-Babili S, et al. Novel carotenoid cleavage dioxygenase catalyzes the first dedicated step in saffron crocin biosynthesis. Proc Natl Acad Sci U S A. 2014:**111**(33): 12246–12251. https://doi.org/10.1073/pnas.1404629111

Goff SA, Klee HJ. Plant volatile compounds: sensory cues for health and nutritional value? Science. 2006:**311**(5762): 815–819. https://doi.org/10.1126/science.1112614

Hou X, Rivers J, Leon P, Mcquinn RP, Pogson BJ. Synthesis and function of apocarotenoid signals in plants. Trends Plant Sci. 2016:**21**(9): 792–803. https://doi.org/10.1016/j.tplants.2016.06.001

Huang FC, Molnar P, Schwab W. Cloning and functional characterization of carotenoid cleavage dioxygenase 4 genes. J Exp Bot. 2009:**60**(11): 3011–3022. https://doi.org/10.1093/jxb/erp137

Ibdah M, Azulay Y, Portnoy V, Wasserman B, Bar E, Meir A, Burger Y, Hirschberg J, Schaffer AA, Katzir N, et al. Functional characterization of CmCCD1, a carotenoid cleavage dioxygenase from melon. Phytochemistry. 2006:**67**(15): 1579–1589. https://doi.org/10.1016/j.phytochem.2006.02.009

Ilg A, Bruno M, Beyer P, Al-Babili S. Tomato carotenoid cleavage dioxygenases 1A and 1B: relaxed double bond specificity leads to a plenitude of dialdehydes, mono-apocarotenoids and isoprenoid volatiles. FEBS Open Bio. 2014:**4**(1): 584–593. https://doi.org/10.1016/j.fob.2014.06.005

Kachanovsky DE, Filler S, Isaacson T, Hirschberg J. Epistasis in tomato color mutations involves regulation of *phytoene synthase 1* expression by *cis*-carotenoids. Proc Natl Acad Sci U S A. 2012:**109**(46): 19021–19026. https://doi.org/10.1073/pnas.1214808109

Kim JE, Yoo HJ, Kang B-C, Lee JM. A new nonsense mutation in capsanthin/capsorubin synthase controlling orange pepper fruit. Hortic Sci Technol. 2017:**35**(5): 599–607. https://doi.org/10.12972/kjhst.20170064

Klee HJ. Improving the flavor of fresh fruits: genomics, biochemistry, and biotechnology. New Phytol. 2010:**187**(1): 44–56. https://doi.org/10.1111/j.1469-8137.2010.03281.x

Klee HJ, Tieman DM. The genetics of fruit flavour preferences. Nat Rev Genet. 2018:**19**(6): 347–356. https://doi.org/10.1038/s41576-018-0002-5

Kloer DP, Ruch S, Al-Babili S, Beyer P, Schulz GE. The structure of a retinal-forming carotenoid oxygenase. Science. 2005:**308**(5719): 267–269. https://doi.org/10.1126/science.1108965

Kohlen W, Charnikhova T, Lammers M, Pollina T, Toth P, Haider I, Pozo MJ, De Maagd RA, Ruyter-Spira C, Bouwmeester HJ, et al. The tomato CAROTENOID CLEAVAGE DIOXYGENASE8 (SlCCD8) regulates rhizosphere signaling, plant architecture and affects reproductive development through strigolactone biosynthesis. New Phytol. 2012:**196**(2): 535–547. https://doi.org/10.1111/j.1469-8137.2012.04265.x

Krinsky NI, Johnson EJ. Carotenoid actions and their relation to health and disease. Mol Aspects Med. 2005:**26**(6): 459–516. https://doi.org/10.1016/j.mam.2005.10.001

Krinsky NI, Landrum JT, Bone RA. Biologic mechanisms of the protective role of lutein and zeaxanthin in the eye. Annu Rev Nutr. 2003:**23**(1): 171–201. https://doi.org/10.1146/annurev.nutr.23.011702.073307

Lashbrooke JG, Young PR, Dockrall SJ, Vasanth K, Vivier MA. Functional characterisation of three members of the Vitis vinifera L. Carotenoid cleavage dioxygenase gene family. BMC Plant Biol. 2013:**13**(1): 156. https://doi.org/10.1186/1471-2229-13-156

Lewinsohn E, Sitrit Y, Bar E, Azulay Y, Ibdah M, Meir A, Yosef E, Zamir D, Tadmor Y. Not just colors—carotenoid degradation as a link between pigmentation and aroma in tomato and watermelon fruit. Trends Food Sci Technol. 2005:**16**(9): 407–415. https://doi.org/10.1016/j.tifs.2005.04.004

Liang MH, Zhu J, Jiang JG. Carotenoids biosynthesis and cleavage related genes from bacteria to plants. Crit Rev Food Sci Nutr. 2018:**58**(14): 2314–2333. https://doi.org/10.1080/10408398.2017.1322552

Lippman ZB, Semel Y, Zamir D. An integrated view of quantitative trait variation using tomato interspecific introgression lines. Curr Opin Genet Dev. 2007:**17**(6): 545–552. https://doi.org/10.1016/j.gde.2007.07.007

Liu JR, Sun XR, Dong HW, Sun CH, Sun WG, Chen BQ, Song YQ, Yang BF. beta-Ionone suppresses mammary carcinogenesis, proliferative activity and induces apoptosis in the mammary gland of the Sprague-Dawley rat. Int J Cancer. 2008:**122**(12): 2689–2698. https://doi.org/10.1002/ijc.23453

Ma G, Zhang L, Matsuta A, Matsutani K, Yamawaki K, Yahata M, Wahyudi A, Motohashi R, Kato M. Enzymatic formation of beta-citraurin from beta-cryptoxanthin and Zeaxanthin by carotenoid cleavage dioxygenase4 in the flavedo of citrus fruit. Plant Physiol. 2013:**163**(2): 682–695. https://doi.org/10.1104/pp.113.223297

Mathieu S, Cin VD, Fei Z, Li H, Bliss P, Taylor MG, Klee HJ, Tieman DM. Flavour compounds in tomato fruits: identification of loci and potential pathways affecting volatile composition. J Exp Bot. 2009:**60**(1): 325–337. https://doi.org/10.1093/jxb/ern294

Downloaded from https://academic.oup.com/plphys/article/192/2/1289/7009207 by Biblioteca Centrale Agraria user on 16 June 2023

Mein JR, Dolnikowski GG, Ernst H, Russell RM, Wang XD. Enzymatic formation of apo-carotenoids from the xanthophyll carotenoids lutein, zeaxanthin and beta-cryptoxanthin by ferret carotene-9′,10′-monooxygenase. Arch Biochem Biophys. 2011:**506**(1): 109–121. https://doi.org/10.1016/j.abb.2010.11.005

Messing SA, Gabelli SB, Echeverria I, Vogel JT, Guan JC, Tan BC, Klee HJ, Mccarty DR, Amzel LM. Structural insights into maize viviparous14, a key enzyme in the biosynthesis of the phytohormone abscisic acid. Plant Cell. 2010:**22**(9): 2970–2980. https://doi.org/10.1105/tpc.110.074815

Mitra S, Estrada-Tejedor R, Volke DC, Phillips MA, Gershenzon J, Wright LP. Negative regulation of plastidial isoprenoid pathway by herbivore-induced β-cyclocitral in Arabidopsis thaliana. Proc Natl Acad Sci U S A. 2021:**118**(10): e2008747118. https://doi.org/10.1073/pnas.2008747118

Monforte AJ, Tanksley SD. Development of a set of near isogenic and backcross recombinant inbred lines containing most of the Lycopersicon hirsutum genome in a L. esculentum genetic background: a tool for gene mapping and gene discovery. Genome. 2000:**43**(5): 803–813. https://doi.org/10.1139/g00-043

Moreno JC, Mi J, Alagoz Y, Al-Babili S. Plant apocarotenoids: from retrograde signaling to interspecific communication. Plant J. 2021:**105**(2): 351–375. https://doi.org/10.1111/tpj.15102

Murray MG, Thompson WF. Rapid isolation of high molecular weight plant DNA. Nucleic Acids Res. 1980:**8**(19): 4321–4325. https://doi.org/10.1093/nar/8.19.4321

Ohmiya A, Kishimoto S, Aida R, Yoshioka S, Sumitomo K. Carotenoid cleavage dioxygenase (CmCCD4a) contributes to white color formation in chrysanthemum petals. Plant Physiol. 2006:**142**(3): 1193–1201. https://doi.org/10.1104/pp.106.087130

Panchy N, Lehti-Shiu M, Shiu SH. Evolution of gene duplication in plants. Plant Physiol. 2016:**171**(4): 2294–2316. https://doi.org/10.1104/pp.16.00523

Pankratov I, Mcquinn R, Schwartz J, Bar E, Fei Z, Lewinsohn E, Zamir D, Giovannoni JJ, Hirschberg J. Fruit carotenoid-deficient mutants in tomato reveal a function of the plastidial isopentenyl diphosphate isomerase (IDI1) in carotenoid biosynthesis. Plant J. 2016:**88**(1): 82–94. https://doi.org/10.1111/tpj.13232

Powell AL, Nguyen CV, Hill T, Cheng KL, Figueroa-Balderas R, Aktas H, Ashrafi H, Pons C, Fernandez-Munoz R, Vicente A, et al. Uniform ripening encodes a golden 2-like transcription factor regulating tomato fruit chloroplast development. Science. 2012:**336**-(6089): 1711–1715. https://doi.org/10.1126/science.1222218

Rambla JL, Medina A, Fernandez-Del-Carmen A, Barrantes W, Grandillo S, Cammareri M, Lopez-Casado G, Rodrigo G, Alonso A, Garcia-Martinez S, et al. Identification, introgression, and validation of fruit volatile QTLs from a red-fruited wild tomato species. J Exp Bot. 2017:**68**(3): 429–442. https://doi.org/10.1093/jxb/erw455

Ramel F, Birtic S, Cuine S, Triantaphylides C, Ravanat JL, Havaux M. Chemical quenching of singlet oxygen by carotenoids in plants. Plant Physiol. 2012:**158**(3): 1267–1278. https://doi.org/10.1104/pp.111.182394

Rodrigo MJ, Alquezar B, Alos E, Medina V, Carmona L, Bruno M, Al-Babili S, Zacarias L. A novel carotenoid cleavage activity involved in the biosynthesis of Citrus fruit-specific apocarotenoid pigments. J Exp Bot. 2013:**64**(14): 4461–4478. https://doi.org/10.1093/jxb/ert260

Romer S, Fraser PD, Kiano JW, Shipton CA, Misawa N, Schuch W, Bramley PM. Elevation of the provitamin A content of transgenic tomato plants. Nat Biotechnol. 2000:**18**(6): 666–669. https://doi.org/10.1038/76523

Rubio-Moraga A, Rambla JL, Fernandez-De-Carmen A, Trapero-Mozos A, Ahrazem O, Orzaez D, Granell A, Gomez-Gomez L. New target carotenoids for CCD4 enzymes are revealed with the characterization of a novel stress-induced carotenoid cleavage dioxygenase gene from Crocus sativus. Plant Mol Biol. 2014:**86**(4–5): 555–569. https://doi.org/10.1007/s11103-014-0250-5

Rubio A, Rambla JL, Santaella M, Gomez MD, Orzaez D, Granell A, Gomez-Gomez L. Cytosolic and plastoglobule-targeted carotenoid dioxygenases from Crocus sativus are both involved in beta-ionone release. J Biol Chem. 2008:**283**(36): 24816–24825. https://doi.org/10.1074/jbc.M804000200

Schauer N, Semel Y, Roessner U, Gur A, Balbo I, Carrari F, Pleban T, Perez-Melis A, Bruedigam C, Kopka J, et al. Comprehensive metabolic profiling and phenotyping of interspecific introgression lines for tomato improvement. Nat Biotechnol. 2006:**24**(4): 447–454. https://doi.org/10.1038/nbt1192

Schmidt H, Kurtzer R, Eisenreich W, Schwab W. The carotenase AtCCD1 from Arabidopsis thaliana is a dioxygenase. J Biol Chem. 2006:**281**(15): 9845–9851. https://doi.org/10.1074/jbc.M511668200

Schwartz SH, Qin X, Loewen MC. The biochemical characterization of two carotenoid cleavage enzymes from Arabidopsis indicates that a carotenoid-derived compound inhibits lateral branching. J Biol Chem. 2004:**279**(45): 46940–46945. https://doi.org/10.1074/jbc.M409004200

Schwartz SH, Tan BC, Gage DA, Zeevaart JA, Mccarty DR. Specific oxidative cleavage of carotenoids by VP14 of maize. Science. 1997:**276**(5320): 1872–1874. https://doi.org/10.1126/science.276.5320.1872

Sharp RE, Lenoble ME, Else MA, Thorne ET, Gherardi F. Endogenous ABA maintains shoot growth in tomato independently of effects on plant water balance: evidence for an interaction with ethylene. J Exp Bot. 2000:**51**(350): 1575–1584. https://doi.org/10.1093/jexbot/51.350.1575

Simkin AJ, Schwartz SH, Auldridge M, Taylor MG, Klee HJ. The tomato carotenoid cleavage dioxygenase 1 genes contribute to the formation of the flavor volatiles beta-ionone, pseudoionone, and geranylacetone. Plant J. 2004:**40**(6): 882–892. https://doi.org/10.1111/j.1365-313X.2004.02263.x

Sun Z, Gantt E, Cunningham FX Jr. Cloning and functional analysis of the beta-carotene hydroxylase of Arabidopsis thaliana. J Biol Chem. 1996:**271**(40): 24349–24352. https://doi.org/10.1074/jbc.271.40.24349

Tan BC, Joseph LM, Deng WT, Liu L, Li QB, Cline K, Mccarty DR. Molecular characterization of the Arabidopsis 9-cis epoxycarotenoid dioxygenase gene family. Plant J. 2003:**35**(1): 44–56. https://doi.org/10.1046/j.1365-313X.2003.01786.x

Tieman DM, Zeigler M, Schmelz EA, Taylor MG, Bliss P, Kirst M, Klee HJ. Identification of loci affecting flavour volatile emissions in tomato fruits. J Exp Bot. 2006:**57**(4): 887–896. https://doi.org/10.1093/jxb/erj074

Tieman D, Zhu G, Resende MF Jr, Lin T, Nguyen C, Bies D, Rambla JL, Beltran KS, Taylor M, Zhang B, et al. A chemical genetic roadmap to improved tomato flavor. Science. 2017:**355**(6323): 391–394. https://doi.org/10.1126/science.aal1556

Umehara M, Hanada A, Yoshida S, Akiyama K, Arite T, Takeda-Kamiya N, Magome H, Kamiya Y, Shirasu K, Yoneyama K, et al. Inhibition of shoot branching by new terpenoid plant hormones. Nature. 2008:**455**(7210): 195–200. https://doi.org/10.1038/nature07272

Van Norman JM, Zhang J, Cazzonelli CI, Pogson BJ, Harrison PJ, Bugg TD, Chan KX, Thompson AJ, Benfey PN. Periodic root branching in Arabidopsis requires synthesis of an uncharacterized carotenoid derivative. Proc Natl Acad Sci U S A. 2014:**111**(13): E1300–E1309. https://doi.org/10.1073/pnas.1403016111

Vogel JT, Tan BC, Mccarty DR, Klee HJ. The carotenoid cleavage dioxygenase 1 enzyme has broad substrate specificity, cleaving multiple carotenoids at two different bond positions. J Biol Chem. 2008:**283**(17): 11364–11373. https://doi.org/10.1074/jbc.M710106200

Vogel JT, Tieman DM, Sims CA, Odabasi AZ, Clark DG, Klee HJ. Carotenoid content impacts flavor acceptability in tomato (Solanum lycopersicum). J Sci Food Agric. 2010a:**90**(13): 2233–2240. https://doi.org/10.1002/jsfa.4076

Vogel JT, Walter MH, Giavalisco P, Lytovchenko A, Kohlen W, Charnikhova T, Simkin AJ, Goulet C, Strack D, Bouwmeester HJ, et al. SlCCD7 controls strigolactone biosynthesis, shoot branching and mycorrhiza-induced apocarotenoid formation in tomato. Plant J. 2010b:**61**(2): 300–311. https://doi.org/10.1111/j.1365-313X.2009.04056.x

Downloaded from https://academic.oup.com/plphys/article/192/2/1289/7009207 by Biblioteca Centrale Agraria user on 16 June 2023

Von Lintig J, Vogt K. Vitamin A formation in animals: molecular identification and functional characterization of carotene cleaving enzymes. J Nutr. 2004:**134**(1): 251S–256S. https://doi.org/10.1093/jn/134.1.251S

Waters MT, Gutjahr C, Bennett T, Nelson DC. Strigolactone signaling and evolution. Annu Rev Plant Biol. 2017:**68**(1): 291–322. https://doi.org/10.1146/annurev-arplant-042916-040925

Yoo HJ, Kim JH, Park KS, Son JE, Lee JM. Light-controlled fruit pigmentation and flavor volatiles in tomato and bell pepper. Antioxidants. 2019:**9**(1): 14. https://doi.org/10.3390/antiox9010014

Yoo HJ, Park WJ, Lee GM, Oh CS, Yeam I, Won DC, Kim CK, Lee JM. Inferring the genetic determinants of fruit colors in tomato by carotenoid profiling. Molecules. 2017:**22**(5): 764. https://doi.org/10.3390/molecules22050764

Ytterberg AJ, Peltier JB, Van Wijk KJ. Protein profiling of plastoglobules in chloroplasts and chromoplasts. A surprising site for differential accumulation of metabolic enzymes. Plant Physiol. 2006:**140**(3): 984–997. https://doi.org/10.1104/pp.105.076083

Zamir D. Improving plant breeding with exotic genetic libraries. Nat Rev Genet. 2001:**2**(12): 983–989. https://doi.org/10.1038/35103590

Zhang B, Liu C, Wang Y, Yao X, Wang F, Wu J, King GJ, Liu K. Disruption of a CAROTENOID CLEAVAGE DIOXYGENASE 4 gene converts flower colour from white to yellow in Brassica species. New Phytol. 2015:**206**(4): 1513–1526. https://doi.org/10.1111/nph.13335

Zhang Y, Cheng X, Wang Y, Diez-Simon C, Flokova K, Bimbo A, Bouwmeester HJ, Ruyter-Spira C. The tomato MAX1 homolog, SlMAX1, is involved in the biosynthesis of tomato strigolactones from carlactone. New Phytol. 2018:**219**(1): 297–309. https://doi.org/10.1111/nph.15131

Zheng X, Zhu K, Sun Q, Zhang W, Wang X, Cao H, Tan M, Xie Z, Zeng Y, Ye J, et al. Natural variation in CCD4 promoter underpins Species-specific evolution of red coloration in Citrus peel. Mol Plant. 2019:**12**(9): 1294–1307. https://doi.org/10.1016/j.molp.2019.04.014

Zhong Y, Pan X, Wang R, Xu J, Guo J, Yang T, Zhao J, Nadeem F, Liu X, Shan H, et al. ZmCCD10a encodes a distinct type of carotenoid cleavage dioxygenase and enhances plant tolerance to low phosphate. Plant Physiol. 2020:**184**(1): 374–392. https://doi.org/10.1104/pp.20.00378

Downloaded from https://academic.oup.com/plphys/article/192/2/1289/7009207 by Biblioteca Centrale Agraria user on 16 June 2023